Digital audio broadcasting : simulations of COFDM and the first field trial at Philips

Steven, S.H.G.

Award date:
1992

FACULTY OF ELECTRICAL ENGINEERING
EINDHOVEN UNIVERSITY OF TECHNOLOGY
TELECOMMUNICATION DIVISION

DIGITAL AUDIO BROADCASTING:

Simulations of COFDM and the first field trial at Philips

by S.H.G. Steven

Report of the graduation work carried out from April 1991 to November 1991 at the Nederlandse Philips Bedrijven, Consumer Electronics, Advanced Development Centre, Broadcasting Laboratory.

Professor : prof. dr. ir. G. Brussaard
Supervisors : ir. C.R. de Graaf (Philips)
ir. A.P. Verlijsdonk

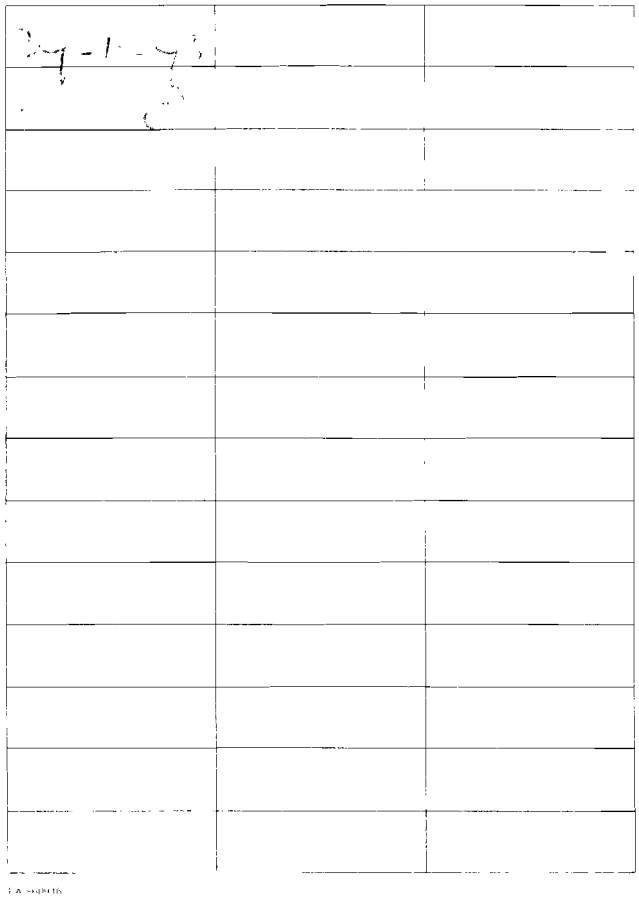

Thanks to:

prof. dr. ir. G. Brussaard
Verlijsdonk, ir. C.R. de Graaf
ing. F. v. d. Laar, ing. G.J. Groeneweg
the Audio Processing Group
and Antonio Vivaldi

ABSTRACT

Mobile reception of FM broadcasting services is quite difficult. Multipath propagation and fading are the major problems. Within the framework of the Eureka 147 project the participants are developing a new digital audio broadcasting system called Digital Audio Broadcasting (DAB). A major starting point was providing an audio quality comparable to that of Compact Disc. A modulation method called Orthogonal Frequency Division Multiplexing (OFDM) has been chosen, which is resistant against multipath propagation. Since the system can deal with multipath propagation, it is possible to use co-channel repeaters in badly served areas, because the signal from the repeater can be seen as an additional reflection.

A transmitter and a co-channel repeater have been installed to test the feasibility of the system. A test vehicle has been provided with a receiver. A measurement setup has been chosen in order to record important channel parameters and the received audio signal while driving. This makes analyzing the data after the test drives possible. The test drives have been carried out both with the repeater turned off and with the repeater turned on.

The system proved to be capable of dealing with multipath reception. The performance of the system is virtually independent of the multipath situation, provided that the impulse response duration does not exceed a certain value, which is determined by the parameters of the modulation system. The limit of operation is, under this condition, solely determined by the field strength. Whenever the field strength was above a certain level, the audio quality was equal to that of a Compact Disc. A co-channel repeater is able to enhance the field strength in a badly served area, which improves the reception quality.

A DAB simulation program has been provided with a model of a mobile channel. Some simulations have been carried out to verify the performance of OFDM. The model provides a basis for studying the effect of different system parameters.

GLOSSARY OF ABBREVIATIONS

ASK	Amplitude Shift Keying
AWGN	Additive White Gaussian Noise
BER	Bit error rate
BPF	Bandpass filter
CCETT	Centre Commun d'Etudes de Télédiffusion et Télécommunications
CD	Compact Disc
COFDM	Coded Orthogonal Frequency Division Multiplexing
DAB	Digital Audio Broadcasting
DAC	Digital to Analog Converter
DAT	Digital Audio Tape
D/A	Digital to Analog
DFT	Discrete Fourier Transform
DPSK	Differential Phase Shift Keying
DQPSK	Differential Quaternary Phase Shift Keying
DR	Direct Recording
DSP	Digital Signal Processor
DSR	Digital Satellite Radio
EIRP	Effective Isotropically Radiated Power
ERP	Effective Radiated Power
HDTV	High Definition Television
IC	Integrated Circuit
IF	Intermediate Frequency
IFFT	Inverse Fast Fourier Transform
ISI	Intersymbol Interference
I/O	Input/Output
FFT	Fast Fourier Transform
FM	Frequency Modulation
MUSICAM	Masking Pattern Universal Subband Integrated Coding And Multiplexing
OFDM	Orthogonal Frequency Division Multiplexing
PC	Personal Computer
PSK	Phase Shift Keying
PTT	Dutch Telecommunication Administration
RF	Radio Frequency
UHF	Ultra High Frequency

GLOSSARY OF SYMBOLS

D_{max}	maximum Doppler frequency
E_b	energy per useful bit
f_k	frequency of carrier k
f_{sample}	sample frequency
j	signalling interval number
k	carrier number
N	number of carriers (emitted + virtual)
N_o	noise power spectral density
T_{sample}	sampling period
T_m	multipath spread or delay spread
T_s	useful symbol duration
T'_s	total symbol duration
Δ	guardband interval duration
$(\Delta f)_{coh}$	coherence bandwidth
$(\Delta t)_{coh}$	coherence time
θ_i	phase shift path i
D_i	Doppler shift path i
θ_i	time delay path i

Contents

1. Introduction

High-quality audio broadcasting started in the 50s with the introduction of FM radio. A decade later stereo operation has been added. The FM system was originally meant for stationary reception with a directional antenna at roof-top level. Nowadays, people expect to receive a signal with a portable or mobile receiver. Under these conditions the reception often is disturbed. Moreover, the introduction of digital sound media, such as Compact Disc (CD) and Digital Audio Tape (DAT), stimulated the demand for high quality sound. This demand is partly met by the introduction of Digital Satellite Radio (DSR) at this moment, which makes stationary radio reception with an excellent sound quality, comparable with CD, possible.

The next step is the development of a terrestrial broadcasting system, suitable for mobile reception and the sound quality delivered must be comparable to that of CD. Within the framework of the European research and development project Eureka 147 a new broadcasting system called Digital Audio Broadcasting (DAB), fully digital from studio to user, is in development. This system uses Orthogonal Frequency Division Multiplex modulation in order to overcome the problems of the mobile channel.

A hardware implementation of a DAB system has been built in order to test the technical feasibility of the system. The first field trial within Philips has been performed. After an introduction to the theoretical aspects of DAB the test method and the results are described in this report.

2. Principles of DAB

In this chapter a brief description of the mobile radio channel will be given. Keeping the properties of the mobile channel in mind, a solution to overcome the problems of the mobile environment will be presented. This solution is the OFDM modulation technique. Once understanding the OFDM modulation technique it is easy to comprehend a method for enhancing the reception quality in not well served areas like tunnels, valleys and heavily shielded urban areas by using gap-fillers.

2.1 Brief description of the mobile channel

The mobile channel is very adverse. The transmitted signal is affected by multipath propagation and the channel characteristics are a function of time. The channel model can be represented by the following block diagram [13]:

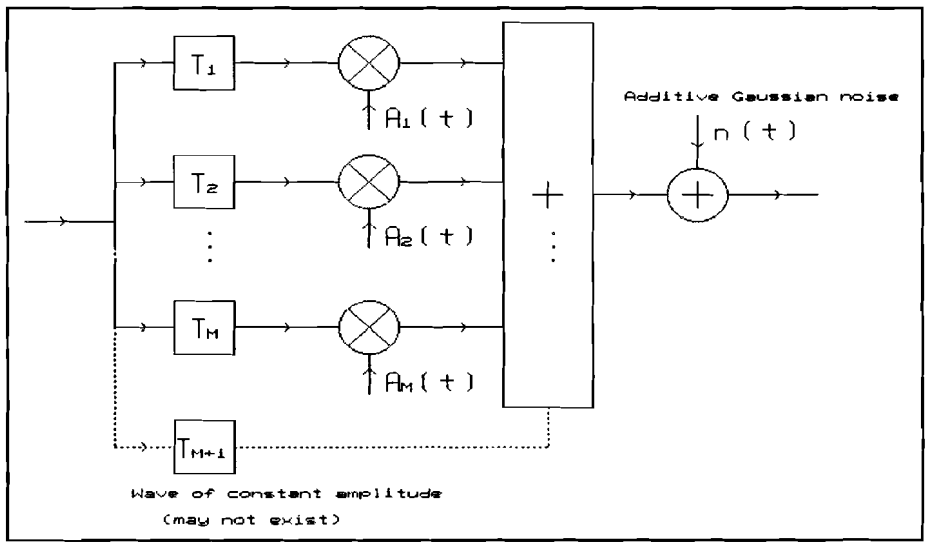

Figure 1. Mobile channel model

The delays T_i arise from specular reflections. The multiplying factors $A_i(t)$ include the effects of local scattering. If the number of scattered waves is large enough, it can be shown that the modulus of the terms $A_i(t)$ follows a Rayleigh distribution [13].

The major problem in a mobile transmission environment is multipath propagation. The channel transfer function is frequency variant and time variant.

The channel impulse response usually extends over a few microseconds. If the multipath delay spread T_m is defined as the spread of the delays T_i in figure 1, then the coherence bandwidth

$$(\Delta f)_{coh} \approx 1/T_m \tag{1}$$

The channel is frequency-selective if the signal bandwidth is larger than $(\Delta f)_{coh}$. If conventional digital modulation systems are used, they will suffer from intersymbol interference (ISI). Given the high selectivity of the channel, conventional equalization techniques are very difficult to implement. If the signalling interval duration T_s satisfies the condition $T_s >> T_m$ the channel introduces a negligible amount of ISI. This condition implies in the frequency domain that $1/T_s << (\Delta f)_{coh}$. If we define a parameter μ

$$\mu = \frac{T_m}{T_s} \tag{2}$$

The condition for a frequency-non-selective channel becomes $\mu << 1$.

The channel being time variant is a consequence of the moving vehicle. A measure of the coherence time of the channel is given by

$$(\Delta t)_{coh} \approx 1/D_{max} \tag{3}$$

D_{max} is the maximum Doppler frequency:

$$D_{max} = v\frac{f}{c} \tag{4}$$

where:

v: *vehicle velocity*
f: *frequency*
c: *speed of light*

The channel attenuation and phase shift are virtually constant when observing

a time duration smaller than the coherence time. The channel is called a time-non-selective (=slowly fading) channel if the channel attenuation and phase shift vary slowly compared to the signalling interval duration T_s. This condition is expressed by

$$T_s \ll (\Delta t)_{coh} \tag{5}$$

Introducing the parameter β:

$$\beta = D_{max} \cdot T_s \tag{6}$$

A channel is time-non-selective if $\beta << 1$.

A modulation method that is able to cope with the problems in a mobile transmission environment is OFDM (Orthogonal Frequency Division Multiplex), provided that the parameters μ and β are properly chosen, namely $\mu < 0.1$ and $\beta < 0.02$ [6]. This modulation method will be described in the next section.

2.2 General principles of OFDM

Narrowband signals are less sensitive to the frequency-selective distortion found in a mobile channel than wideband signals. Instead of modulating the data (bitrate r_b) onto a single carrier, the OFDM system uses a large number N of (D)PSK-modulated carriers [2], each having a low bitrate (r_b/N). The bit duration of each carrier (N/r_b) is N times longer than the bit duration in the case of a single carrier ($1/r_b$), so the transmission suffers less from ISI.
On the other hand the bitrate of each carrier must have a certain minimum value, which is determined by the coherence time, otherwise we are confronted with the problem of fast fading. This is very unfavourable in the case of differential PSK.

Let $\{f_k\}$ be the set of carrier frequencies, with:

$$f_k = f_0 + k/T_s,\ k = 0\ to\ N-1 \tag{7}$$

where k represents the number of the carrier and T_s the time duration of the symbol ($T_s = N/r_b$). An orthogonal base of signals is then defined as

$$\Psi_{j,k}(t) = g_k(t - jT_s),\ with\ k = 0\ to\ N-1,\ j = -\infty\ to\ \infty$$

$$where:$$

$$g_k(t) = \exp^{2i\pi f_k t} \qquad 0 \le t \le T_s$$
$$g_k(t) = 0 \qquad otherwise \tag{8}$$

The signal spectra of $g_k(t)$ mutually overlap. The sum of all these overlapping spectra approximates a rectangular spectrum.

The set of signals $\Psi_{j,k}(t)$ satisfies the orthogonality conditions:

$$\int_{-\infty}^{+\infty} \psi_{j,k}(t)\psi^*_{j',k}(t)dt = 0 \quad j \neq j'\ or\ k \neq k'$$

$$and \tag{9}$$

$$\int_{-\infty}^{\infty} \|\psi_{j,k}(t)\|^2 dt = T_s$$

where "*" represents the complex conjugate and $\|.\|$ the modulus of a complex number.

The modulated OFDM signal can then be written (complex representation)

$$x(t) = \sum_{j=-\infty}^{+\infty} \sum_{k=0}^{N-1} C_{j,k}\Psi_{j,k}(t) \tag{10}$$

The complex symbol $C_{j,k}$ represents the phase modulation. If each carrier is QPSK modulated then $C_{j,k}$ is selected from the alphabet { 1+i, 1-i, -1+i, -1-i }.

The demodulation rule may be expressed as

$$C_{j,k} = \frac{1}{T_s}\int_{-\infty}^{+\infty} x(t)\Psi_{j,k}^{*}(t)dt \qquad (11)$$

The spectra of the N modulated carriers mutually overlap, but the orthogonality conditions (9) guarantee that the data of each carrier can be extracted without mutual interference between the N carriers.

The spectrum of the OFDM-signal is presented in figure 2 (Y-axis in dB, X-axis in Hz). The carriers are QPSK modulated. The number of carriers is 16 and the symbol duration $T_s = 64$ µs.

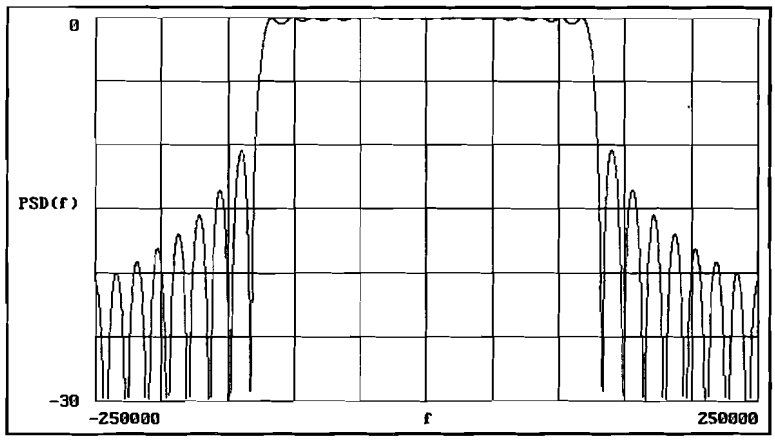

Figure 2. The OFDM spectrum

2.3 Utilisation of a guard interval

In the case of multiple paths in the transmission channel the condition of perfect orthogonality between the N signals is no longer maintained, resulting in mutual interference between the N signals. A solution would be increasing indefinitely the number of carriers and the symbol duration. But besides from

technological limitations, there would arise the problem of fast-fading: the channel characteristics change during one signalling interval. The solution comprises the addition of a guard interval before each useful symbol. If the guard interval duration is longer then the spread of the impulse response of the channel, the useful period of the signal remains free of ISI.

Let

$$T_s' = T_s + \Delta$$

where:

T_s: *useful symbol duration*
Δ: *guard interval duration*
T_s': *total symbol duration*

(12)

The useful signals are defined by

$$\Psi_{j,k}(t) = g_k(t - jT_s') \tag{13}$$

The base of elementary signals becomes

$$\Psi_{j,k}(t)' = g_k'(t - jT_s), \text{ with } k = 0 \text{ to } N-1,\ j = -\infty \text{ to } \infty$$

where

$$g_k'(t) = \exp^{2i\pi f_k t} \qquad -\Delta \le t \le T_s$$
$$g_k'(t) = 0 \qquad \text{otherwise} \tag{14}$$

The modulated OFDM signal can then be written as

$$x(t) = \sum_{j=-\infty}^{+\infty} \sum_{k=0}^{N-1} C_{j,k} \Psi_{j,k}'(t) \tag{15}$$

The decoding rule can be deduced as

$$C_{j,k} = \frac{1}{T_s} \int_{-\infty}^{+\infty} x(t) \Psi_{j,k}^*(t) dt \tag{16}$$

The use of a guard interval causes the spectrum of the OFDM-signal to be non-white (figure 3). The guard interval duration is 16 μs and the useful symbol duration is 64 μs. The number of carriers is 16.

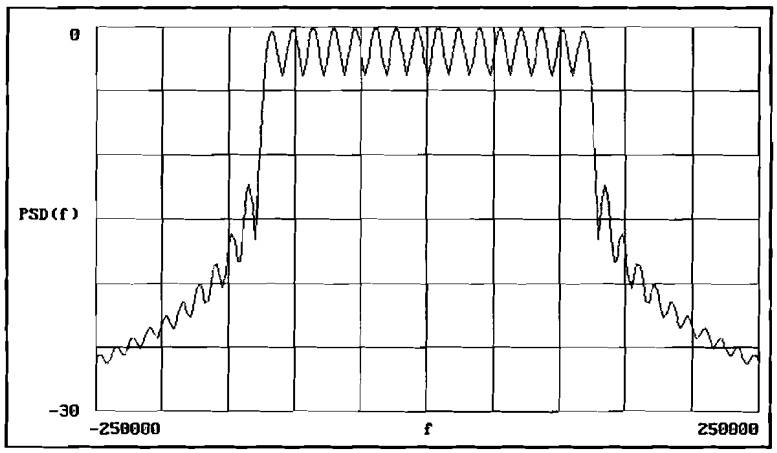

Figure 3. The spectrum of the OFDM-signal with guard interval.

2.4 The OFDM system in the presence of multipath propagation

For the analysis we assume that the following conditions are valid:

- the duration of the channel impulse response T_m is less than Δ.
- the channel varies slowly compared with the symbol duration T'_s.

Under these conditions it is possible to describe the multipath channel by a set of discrete values $H_{j,k}$ representing the complex response at the frequency f_k and at the instant jT'_s:

$$H_{j,k} = \rho_{j,k} e^{i\varphi_{j,k}} \tag{17}$$

Under these conditions the useful signal is not affected by intersymbol interference. The received signal can then be written as

$$y(t) = \sum_{k=0}^{N-1} H_{j,k} C_{j,k} \Psi_{j,k}(t) \quad jT'_s \le t < jT'_s + T_s \tag{18}$$

If we apply the decoding rule (10) we obtain the transmitted $C_{j,k}$ multiplied by

the channel response:

$$H_{j,k}C_{j,k} = \frac{1}{T_s}\int_{-\infty}^{+\infty} y(t)\Psi_{j,k}^{*}(t)dt \qquad (19)$$

Differential modulation/demodulation can be applied, because the channel frequency transfer function ($H_{j,k}$) changes slowly compared with the symbol duration ($C_{j,k}$). So the system is able to cope with multipath propagation if the duration of the impulse response is less than the duration of the guard interval.

2.5 Demodulation of the OFDM-signal

The conventional method of demodulating the OFDM-signal is the use of matched filters: for each of the emitted carriers f_k, a filter matched to the signal $g_k(t)$ is necessary. Because of the orthogonality of the signals $g_k(t)$ the demodulation can be performed by using FFT operations.
The received signal is translated to baseband by means of mixing with a local oscillator of the frequency $f_o+1/2T_{sample}$, with $T_{sample}=T_s/N$. The complex baseband signal can be written:

$$\begin{aligned} y_b(t) &= \sum_{k=0}^{N-1} H_k C_k e^{2i\pi f_k t} \times e^{-2i\pi(f_0+1/2T_{sample})t} \\ &= e^{-i\pi t/T_{sample}} \sum_{k=0}^{N-1} H_k C_k e^{2i\pi kt/NT_{sample}} \end{aligned} \qquad (20)$$

The baseband signal is converted into a train of samples. The baseband signal is sampled at a frequency $f_{sample}=1/T_{sample}$:

$$y_b(nT_{sample}) = (-1)^n \sum_{k=o}^{N-1} H_k C_k e^{2i\pi kn/N} \qquad (21)$$

Let us write

$$y_n = \frac{(-1)^n}{N} y_b(nT_{sample}) \text{ and } Y_k = H_k C_k \tag{22}$$

Thus we have

$$y_n = \frac{1}{N} \sum_{k=0}^{N-1} Y_k e^{2i\pi kn/N} \tag{23}$$

$\{y_n\}$ appears as the inverse discrete Fourier transform (IDFT) of $\{Y_k\}$. Y_k can thus be calculated by using a FFT algorithm:

$$Y_k = \sum_{n=0}^{N-1} y_n e^{-2i\pi nk/N} \tag{24}$$

The sampling frequency f_{sample} should be more than twice the maximum frequency of the baseband signal $y_b(t)$ (Nyquist). This is satisfied by choosing $f_{sample}=1/T_{sample}$. Since rectangular filter characteristics are not realisable we choose $f_{sample}=1/T_{sample}$ and we limit the number of emitted carriers to N_{active} which is less than N, in order to reduce the bandwidth slightly.

In a practical transmitter the modulation is done by calculating an IFFT of the phases, which are represented by the complex numbers C_k. The output of the IFFT is passed trough a D/A converter. At the output of this converter an OFDM baseband signal is available [18].

2.6 Channel coding

The decrease of the bit error rate as a function of the transmitted power in a Rayleigh channel is very slow (in Appendix F some BER curves are given). By using a coding/decoding scheme (COFDM, Coded OFDM) we have a virtually error free system if the signal strength at the receiver is above some threshold.

Due to the nature of the mobile channel errors occur in bursts. There is a dependency between successive channel bits. Codes of the algebraic type are

capable of correcting burst errors, but the implementation is very complex. Convolution codes together with soft-decision Viterbi decoding are easier to implement, but independence between successive bits at the Viterbi decoder input has to be guaranteed. This independence is created by applying interleaving schemes. This interleaving is done in two dimensions, namely interleaving in time and interleaving in frequency.

2.7 Interleaving

We have stated that the conditions of independence are created by the use of interleaving.

Time interleaving is useful for mobile reception. If a deep fade occurs, there will be an error burst in the channel bitstream. But after de-interleaving in the receiver, this burst will be spread out in time.

Frequency interleaving is necessary for stationary reception. If the channel transfer function has a dip affecting a number of adjacent carriers, the use of frequency interleaving/de-interleaving spreads this errorburst: without frequency interleaving the data of adjacent carriers are presented sequentially at the decoder.

In figures 4 and 5 an example of an interleaving scheme is presented. The time interleaving depth is 8. The number of carriers is also 8. The interleaving schemes are based on a bitreversed ordering. The delays in the time interleaving schemes are expressed in numbers of frames. The meaning of a frame is explained in chapter 3. At this point it is sufficient to state that the delay time durations are the numbers given in the figures multiplied by 24 ms, being the frame duration.

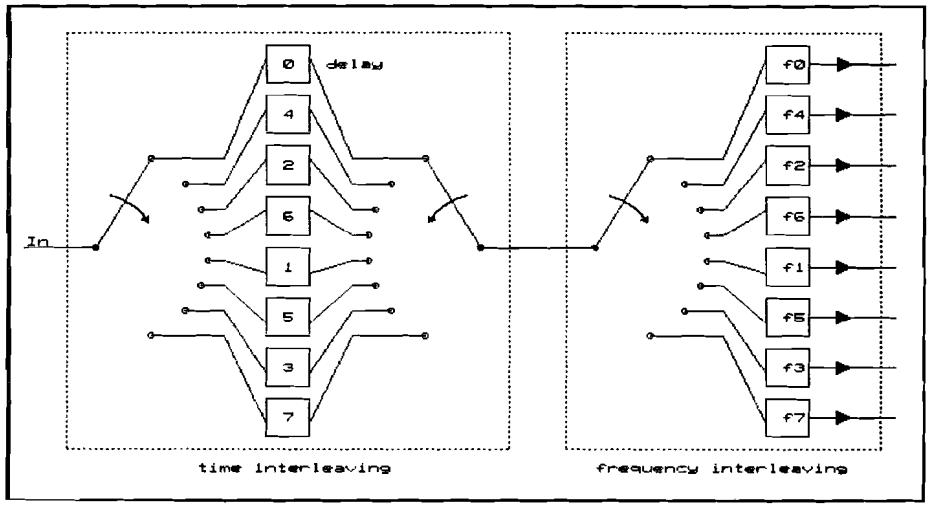

Figure 4. Time and frequency interleaving.

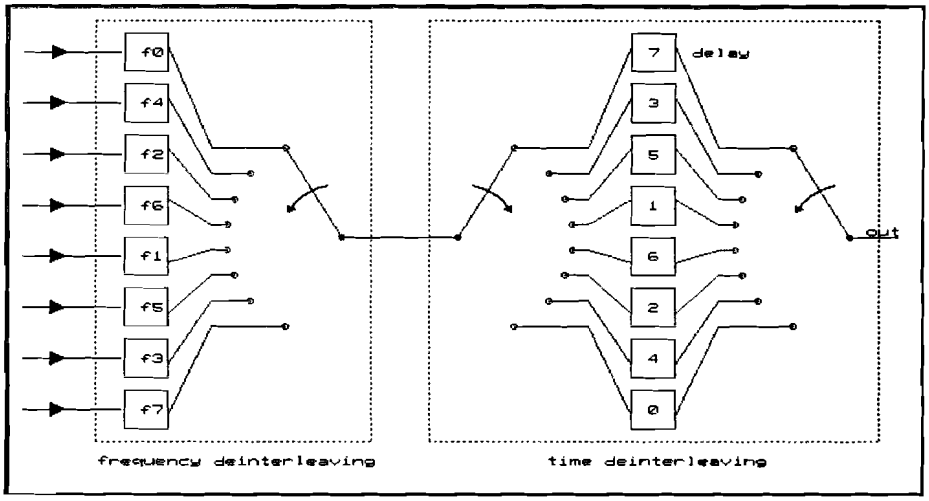

Figure 5. Time and frequency de-interleaving.

A practical value for the time interleaving depth is 16, a practical value for the number of frequencies is 512. The carriers depicted in the frequency interleaving and de-interleaving blocks are not physically present in a practical system. Frequency interleaving at the transmitter is done by bitreversing the order of the data presented at the IFFT. In the receiver frequency de-interleaving is done by bitreversing the order of the data at the output of the FFT.

A consequence of the use of time interleaving is a system delay, which is in this

case 15 times 24 ms = 360 ms.

2.8 Gap-filler

We have seen that a feature of the OFDM system is the ability to make constructive use of multipath reflections, provided that the multipath spread does not exceed the guard interval duration. This means that it is possible to use a co-channel relay (gap-filler) at an area which is not well served by the main station. Such a relay consists of a receive antenna (at a high level above ground), an amplifier and a transmit antenna (figure 6).

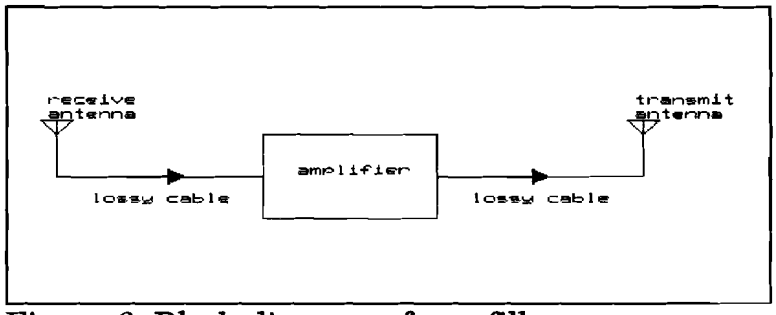

Figure 6. Block diagram of gap-filler.

Since a relay has an internal delay of a few microseconds, this causes an extra reflection during the reception of a OFDM-signal in the neighbourhood of the gap-filler. The OFDM-receiver is able to make constructive use of the received echo.

In order to make filtering of the received signal easy, the received signal is converted to an IF signal. This IF signal is fed through a bandpass filter. The output of the bandpass filter is converted back to a RF signal by using the same local oscillator. This guarantees that the frequency of the output signal is

equal to the frequency of the input signal. In figure 7 a block diagram of an amplifier is given.

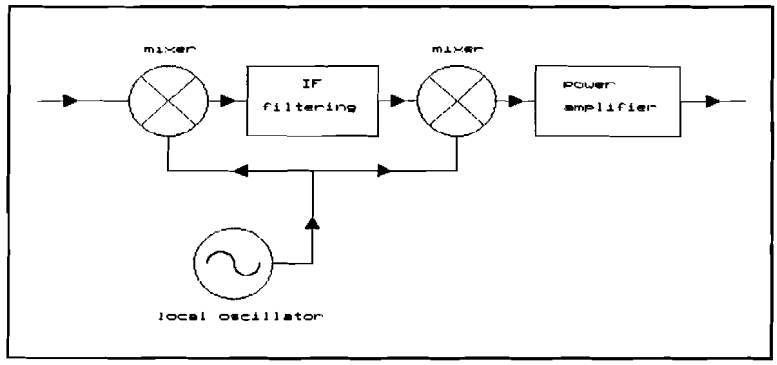

Figure 7. Block diagram of gap-filler amplifier.

2.9 Source coding

A CD stereo signal using a sample frequency of 44.1 kHz and 16 bits per sample produces a bitrate as high as 1.4 Mbit/sec. Since one of the main targets of the DAB-project is the development of a new broadcasting system with a spectral requirement comparable to FM, it is evident that a drastic bitrate reduction is needed. However, the subjective audio quality must be comparable to that of CD. A method for realising this objective is the *M*asking Pattern *U*niversal *S*ubband *I*ntegrated *C*oding *A*nd *M*ultiplexing (MUSICAM) sub-band audio coding technique. This method is implemented in the DAB system under test.

The sub-band coding technique is based on the psycho-acoustic properties of the human ear. The irrelevant audio information is eliminated by taking advantage of masking effects in the human auditory system. An illustration of a masking effect is given in figure 8.

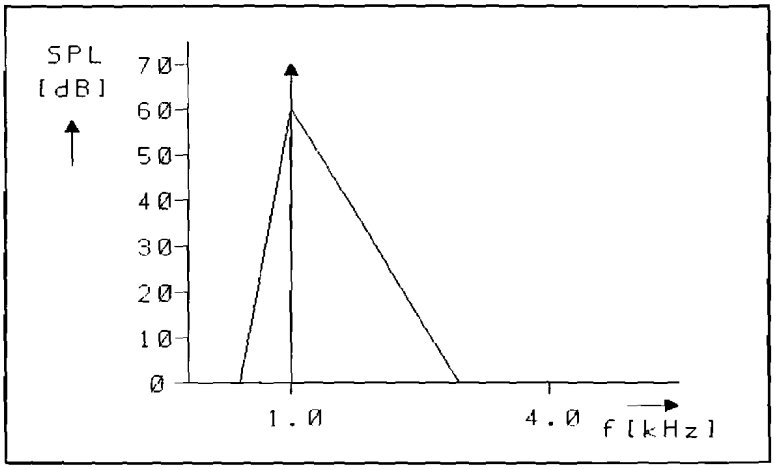

Figure 8. Masking threshold.

If we feed for instance a tone of 1 kHz with 70 dB Sound Pressure Level (SPL) to the human ear, then all additional frequency components having a SPL beneath the triangle are not perceived. We make use of this property of the human ear by dividing the audio spectrum into a number of subbands. Each sub-band is quantised individually. Some sub-bands need to be quantised with less than 2 bits/sample. The average number of bits per sample needed, is about 3⅓. This achieves a reduction in bitrate of a factor 5. A further reduction can be achieved by taking into account the masking between sub-bands, in stead of the masking within each sub-band only: the peak level occurring in a 8 ms slot is determined for each sub-band and a 'scale-factor' is assigned to each sub-band. The quantising level is not fixed, so the scale-factors are transmitted together with the samples. The bit reduction is increased further: 7 times. So it is possible to code and decode a stereo audio signal using a bitrate of 200 kbit/s, while maintaining the subjective audio quality.

3. Parameters of the DAB system under test

In this chapter the parameters of the transmitter station, the gap-filler and the test vehicle will be summarised. The DAB transmission parameters given here, are the parameters of the first generation hardware. This system will probably not be the definitive system to be used in the future, but this system is used for testing because this system is available in hardware.

3.1 DAB transmission parameters

The CCETT has proposed four DAB-systems. The system used for testing the performance of OFDM under real conditions is system 2. The parameters of system 2 are presented in table 1:

Table 1: system parameters of system 2

Total number of carriers	512
Total number of useful carriers	448
Carrier spacing	15625 Hz
Useful symbol duration	64 µs
Guard interval duration	16 µs
Nominal bandwidth	7 MHz
Modulation	QPSK
Channel coding	Convolutional
Rate	1/2
Free distance	10
Channel decoding	Max. likelihood Viterbi decoder 4 bit soft decision

The system under test was provided with the MUSICAM audio coding system.

The parameters of the implemented version of MUSICAM are given in table 2.

Table 2. Parameters of MUSICAM

Bitrate per stereo channel: - total bit-stream - samples and scalefactors - error protection	 320 kbit/s 277.4 kbit/s 42.6 kbit/s
Number of sub-bands:	32
Width of sub-bands	500 Hz
Sampling rate:	48 kHz
Block length:	8 ms
Error protection: - code - covering	 - Golay - scale-factors and bit allocation

These are the parameters of layer 1. This version is used in the field trials.

In figure 9 a diagram of the complete DAB system is given.

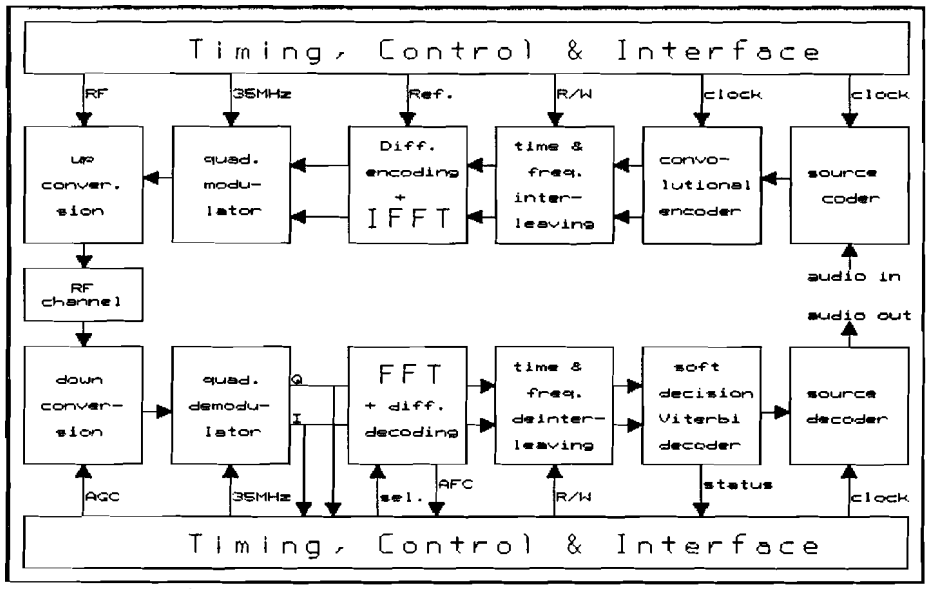

Figure 3. DAB system.

The signal is built up around a 24 ms frame structure corresponding to the juxtaposition of 300 symbols (Figure 10)

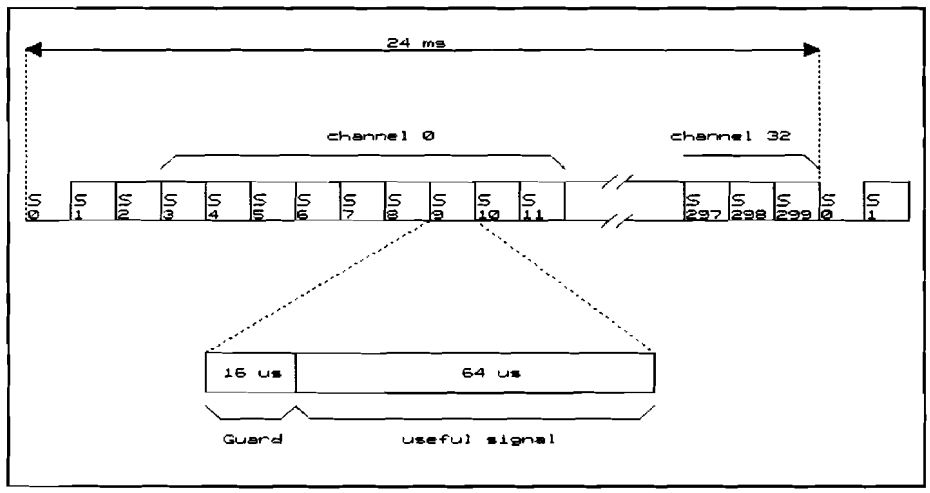

Figure 10. System 2 frame structure.

The first symbol of the frame (S_0) is the null symbol. The null symbol is free of modulation and is used to roughly synchronize the receiver and prepositioning the FFT window. The second symbol is a sine sweep signal, which is the phase

reference for the differential modulation. Besides, this symbol is used for estimating the channel impulse response and refining the position of the FFT window. The third symbol carries static data. The remaining 297 symbol are divided into 33 channels. Each channel consists of 9 symbols. The first channel (channel 0) is a data broadcasting channel. The remaining 32 channels correspond to 32 monophonic sounds.

3.2 DAB transmitting station parameters

The DAB transmitter is located at the Philips research laboratory in Eindhoven. In figure 11 a diagram of the DAB transmitting station is given.

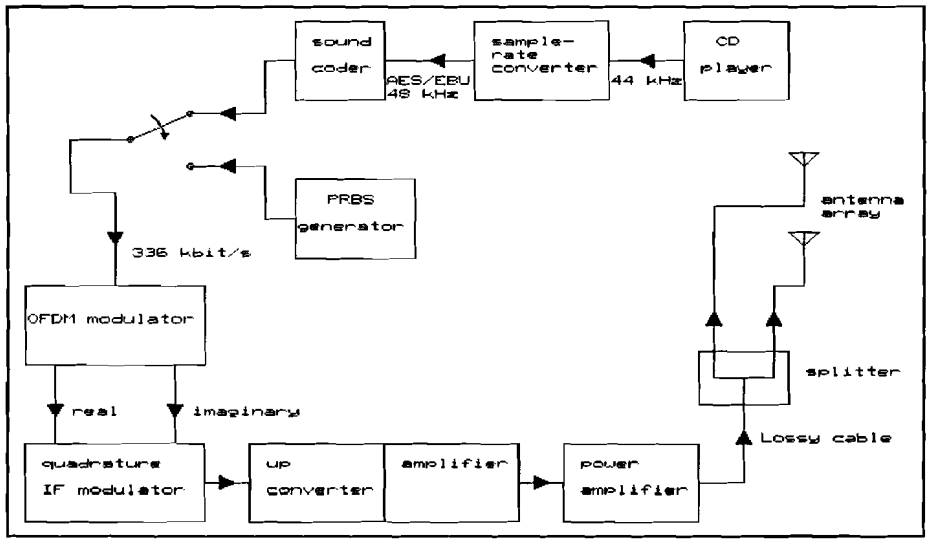

Figure 11. DAB transmitter station.

The power at the output of the quadrature modulator (1) is 0.08 mW at 50Ω. This is an IF signal at 35.075 MHz. The upconverter/amplifier converts the IF signal to an RF signal at 762 MHz, TV channel 57. This signal is fed to a power amplifier. The power amplifier output power is 8 W. The cable loss is 3 dB, so the power at the input of the power splitter is 4 W. The power splitter is a Kathrein K63604A. The datasheet is given in Appendix A.

The antenna consists of two Kathrein K733147 antennas on top of each other. The datasheets are given in Appendix B. Appendix B.1 is the general datasheet. Appendix B.2 gives the horizontal radiation pattern for the frequency range we used. The horizontal radiation pattern is valid for one antenna and for the antenna array. The vertical radiation pattern of the array is given in Appendix B.3. The gain of one antenna is 11 dBd (ref. to a $\lambda/2$ dipole). The use of an antenna array, consisting of two elements, gives an extra gain of 3 dB. The gain of the antenna array is therefore 14 dBd = 25. The effective radiated power is 100 W_{ERP} = 164 W_{EIRP}. The effective radiated power per stereo program is therefore 6.25 W_{ERP} = 10.25 W_{EIRP}. The polarisation is vertical. The antenna height is approximately 65 m above ground level. The 3 dB beamwidth is approximately 52 degrees. The first zero in the vertical radiation pattern corresponds to a distance of 365 m for the given antenna height. In Appendix C a map of Eindhoven is given containing the 3 dB antenna beam.

3.3 Gap-filler parameters

The gap-filler is located at the building of electrical engineering of the Eindhoven University of Technology. The receive antenna is located at the south side of the building. The height of the transmit antenna is estimated at 75 m above ground level. The transmit antenna is mounted on the roof at the north side of the building. Both antennas are made by Kathrein, number K722347. Appendix D contains the datasheet of the antenna. The gain of the antenna is 8.5 dB = 7. The required power at the input of the antenna is 0.7 W, yielding an ERP of 5 W (= 8.2 W_{EIRP}). The loss of the cable between amplifier and antenna is 3.1 dB. Therefore the power at the output of the amplifier has been fixed at 1.4 Watt (31.5 dBm).

The power at the output of the receive antenna in dB is given by

$$P_{re} = P_{tr} + G_{tr} + G_{re} - L$$

where:

P_{re}: *power at output of gap-filler receive antenna*
P_{tr}: *power at input of NatLab transmit antenna*
G_{tr}: *gain of transmit antenna*
G_{re}: *gain of receive antenna*
L: *basic transmission loss*

(25)

The basic transmission loss is given by the free space loss plus the medium loss, which is taken to be zero:

$$L = 32.45 + 20\log d_{(km)} + 20\log f_{(MHz)}$$

where:

(26)

d: *distance between transmitter and receiver* (≈4.8 *km*)
f: *frequency* (=762 *MHz*)

The received power can now be calculated

$$P_{re} = 36 + (14 + 2.15) + (8.5 + 2.15) - (32.45 + 13.6 + 57.6) \approx -41 \ dBm \qquad (27)$$

Note that the isotropic antenna gains are used (the gain of a λ/2 dipole is 2.15 dB referred to an isotropic radiating antenna).
The loss of the cable between receiving antenna and the amplifier is 4.95 dB (measured by the PTT). The power at the input of the amplifier is therefore -45 dBm. The required amplification is 45 dB + 31.5 dB = 76.5 dB. The amplification has been measured by the PTT. The result was 79 dB. This result can be explained by the fact that the medium loss has been omitted in the calculation.

3.4 Test vehicle parameters

The test vehicle is a Mercedes 210 van. This van is owned and maintained by Car Stereo. The van is provided with a worktable at which two persons can

have a seat.

The car is provided with an extra battery (12 Volt, 88 Ah) and a more powerful dynamo of 80 A, instead of 55 A. The extra battery is connected to the original battery by a relay, which is opened if the engine is off. The battery is connected to a DC/AC converter. At the output of this converter there's 220 V/50 Hz (500 VA) available. The converter type is a EA-MEC 505/12.

In figure 12 a diagram of the receiver front end is given.

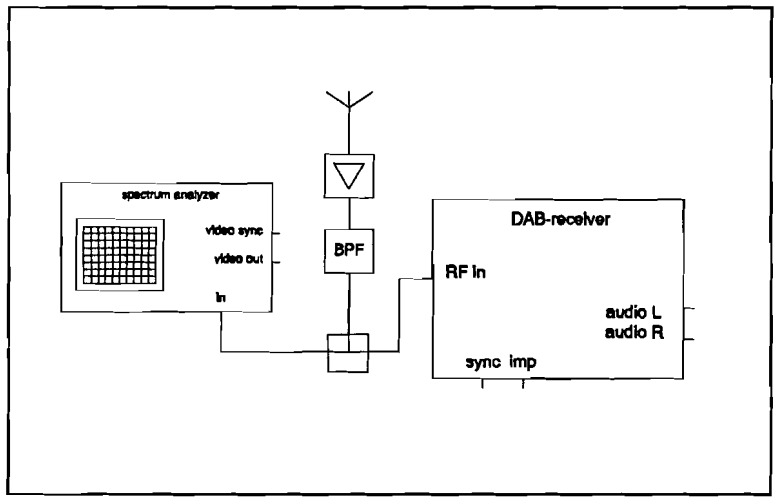

Figure 12. Diagram of receiver front end.

The receiving antenna is a $\lambda/4$ groundplane antenna, which is placed at the roof of the van. The exact gain of this antenna is unknown, it has not been found in the literature. However, the gain of this antenna is situated between the gain of a dipole and the gain of a Marconi antenna. The gain of this antenna is estimated at 3 dB. The output of the antenna is connected to a preamplifier with a gain of 9 dB. The signal at the output of the preamp is passed to a bandpass filter (type LHB2066) via a 1 m long coaxial cable (RG58C, loss 0.5 dB/m). The output of the bandpass filter is connected via a 30 cm long coaxial cable to a splitter. The splitter is connected to the DAB-receiver and to a spectrum analyzer, both via a 30 cm long coaxial cable. The total cable loss (input and output bandpass filter, and input and output splitter) is estimated

at 1 dB. The bandpass filter attenuation in the passband is 5 dB. The spectrum analyzer is used in order to monitor the spectrum of the received signal. The need of the spectrum analyzer will be described in a following chapter. The frequency response of the filter is given in Appendix E. Two curves are given: the original curve and the curve after the filter had been adjusted by Car Stereo. The line out of the DAB-receiver is connected to 4 headphone amplifiers, each amplifier having an individual volume control.

3.5 Theoretical range of main transmitter and gap-filler

According to the CCETT specifications the BER at the output of the Viterbi decoder is smaller then 10^{-2} if the RF input level of the DAB-receiver is between -92 dBm and -30 dBm . This also is the maximum BER at which the audio decoder can stay in operation. The sensitivity of the DAB-receiver is therefore -92 dBm.

The calculation of the service area is based on the Okumura model [21]. The model predicts a minimum field strength for a certain percentage of the locations. In order to make use of the model, it is necessary to derive a relation between the field strength and the power at the output of the receive antenna. The derivation is based on the free space model. However, the relation between the field strength and the power at the output of the receive antenna which will be derived, is always valid.

The power density S is given by

$$S = \frac{E_{eff}^2}{120\pi} \quad [W/m^2] \tag{28}$$

where:
E_{eff}: *the effective field strenght* [*V/m*]

The power density at a distance d in m is given by

$$S = \frac{G_{tr} P_{tr}}{4\pi d^2} = \frac{EIRP}{4\pi d^2} \tag{29}$$

where:

G_{tr} : *isotropic gain of transmit antenna*
P_{tr} : *power at the input of transmit antenna* [*W*]
d : *distance* [*m*]
$EIRP$: *effective isotropically radiated power* [*W*]

Combining (28) and (29) leads to the following expression for the field strength in V/m at a distance d in m as a function of the EIRP:

$$E_{eff} = \frac{\sqrt{30\, EIRP}}{d} = \frac{\sqrt{30 \cdot 1.64 \cdot ERP}}{d} \tag{30}$$

The power at the output of the receive antenna is given by

$$P_{re} = \frac{EIRP\, G_{re}}{\left(\frac{4\pi d}{\lambda}\right)^2}$$

where:

G_{re} : *isotropic gain of receive antenna*
λ : *wave lenght* [*m*]

Combining the expressions for P_{re} and E_{eff} leads to the following relation between the field strength and the power at the output of the receive antenna:

$$P_{re} = \frac{1}{30}\left(\frac{\lambda}{4\pi}\right)^2 G_{re} E_{eff}^2 \tag{32}$$

Using f=762 MHz and G_{re} = 3 dB = 2 leads to

$$P_{re} = 6.5 \times 10^{-5} E_{eff}^2 \tag{33}$$

The loss between receive antenna and receiver is the sum of the loss of cable, bandpass filter and splitter minus the amplifier gain, that is respectively 1 dB, 5 dB, 3 dB and -9 dB = 0 dB. The power at the output of the receive antenna P_{re} is equal to the power at the input of the receiver.

The sensitivity of the receiver is -92 dBm. This corresponds to a field strength $E_{eff} = 9.84 \times 10^{-5}$ V/m. E_{eff} is usually expressed in dBµV/m:

$$E_{eff} = 20 \log \left(\frac{E_{eff}\ [V/m]}{10^{-6}\ [V/m]} \right) \quad \left[\frac{dB\mu V}{m} \right] \tag{34}$$

The receiver sensitivity expressed in dBµV/m is therefore 40 dBµV/m.

The Okumura curves (figure 13) show the field strength exceeded at 50% of the locations.

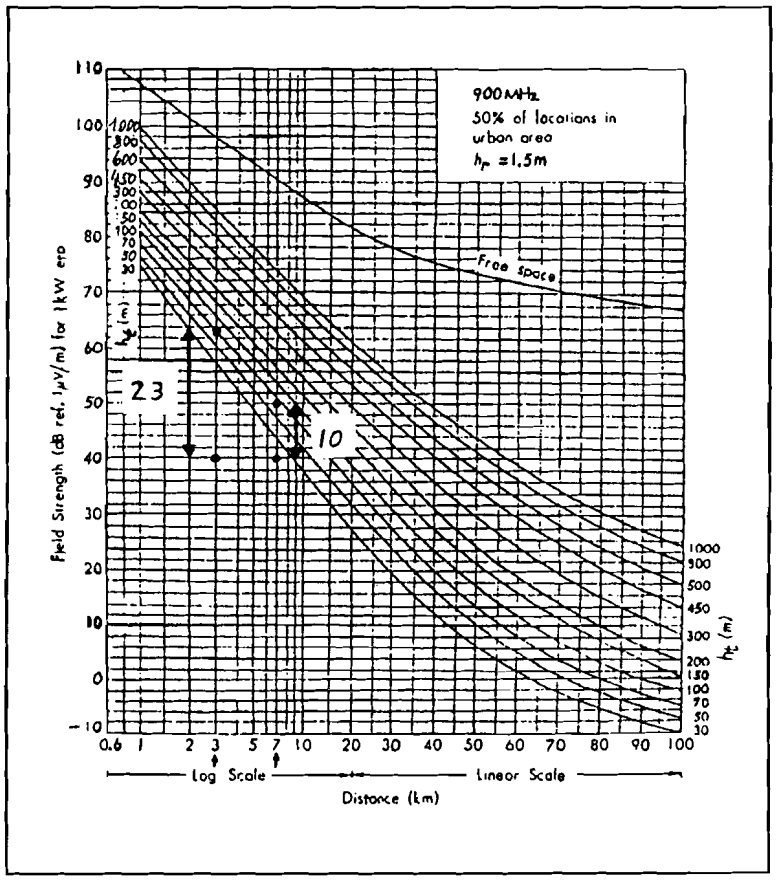

Figure 13. Okumura model.

The percentage of the locations is 50%, because 50% of the locations covered at the edge of the service area is the target for FM. A higher percentage is preferred, but this is the only model found which applies to distances smaller than 10 km.

The ERP of the main transmitter is 100 W and the ERP of the gap-filler is 5 W. The curves are given for an ERP of 1 kW. Therefore the curves have to be shifted down for 100 W and 5 W by 10 dBμV/m and 23 dBμV/m respectively. The curves for 762 MHz and 900 MHz are expected to be virtually identical. We therefore conclude that the range for the main transmitter is 7 km (within the beam of the transmit antenna) for 50% of the locations. The range of the gap-filler alone is 3 km (within the beam of the gap-filler transmit antenna).

4. Simulations of the performance of OFDM

A DAB simulation program, which has been developed at Philips, has been provided with a Gaussian and a Rayleigh channel model. This program is used for simulating the performance of the OFDM system.

4.1 DAB simulation program

At Philips a DAB simulation program had been written previously in PASCAL. This program was mainly used to verify the knowledge on the implementation of DAB building blocks. The mobile radio channel was not implemented in the program. A mobile radio channel model and a user interface has been added. Furthermore a number of additional functions have been added, for instance a function which performs the calculation of the BER, functions for calculating the frequency response and the impulse response of the channel, a function which generates a Gaussian random variable faster.

The OFDM signal is a set of N DQPSK modulated carriers. These carriers are generated by using an IFFT: the IFFT is carried out on N complex numbers, $C_k=A_k+jB_k$, k:0..N-1, which represent the phases of the N carriers. The IFFT converts the N complex numbers to a time discrete version of the OFDM signal. This time discrete version consists of N complex samples, a_i+jb_i, i:0..N-1 . In a real transmitter these samples are presented to a Digital to Analog Converter (DAC). This analogue signal is then modulated at a high frequency carrier.

The mobile channel model used in the computer simulations operates solely on the time discrete version of the OFDM signal, so the mobile channel model is a baseband time discrete channel model. A detailed description of the program is given in Appendix A.

4.2 Channel modelling

4.2.1 Gaussian channel

The simplest channel is the Gaussian channel. The received signal is corrupted with Additive White Gaussian Noise (AWGN). This means a random variable with a Gaussian probability density function has to be added to every a_i and b_i. The variance of the Gaussian variable depends on E_b and on E_b/N_o. E_b is the energy per useful bit, which is equal to the ratio of the transmitted power and the useful bitrate. E_b/N_o is the ratio of the energy per useful bit and the noise power spectral density. The useful bits are defined as the bits prior to the convolutional encoder (and of course at the output of the Viterbi decoder). E_b can be written as

$$E_b = \sum_{i=0}^{N-1} \frac{a_i^2 + b_i^2}{N} \tag{35}$$

N is the number of carriers (emitted +virtual), which is equal to the number of samples per symbol. If a guard interval is used, then (35) is multiplied by T'_s/T_s. In this program the modulus of A_k+jB_k is equal to one. The IFFT function which is implemented in the simulation program, multiplies the energy by N, so in this program E_b is equal to N.
The noise variance can be calculated as

$$\sigma^2 = \frac{N_o}{2} = \frac{1}{2}\left(\frac{Eb}{N_o}\right)^{-1} E_b \tag{36}$$

The proof of $\sigma^2=N_o/2$ is given in [1]. If E_b/N_o is expressed in dB then E_b/N_o can be written as

$$\frac{E_b}{N_o} = 10^{\frac{(E_b/N_o)_{dB}}{10}} \tag{37}$$

Finally, the noise variance can be calculated as

$$\sigma^2 = \frac{E_b}{2 \cdot 10^{\frac{(E_b/N_o)_{dB}}{10}}} \tag{38}$$

This formula is implemented in the program.

4.2.2 Rayleigh channel

In chapter 2 a brief description of the mobile radio channel is given. Now the mobile radio channel is described in detail.

The mobile radio channel is affected by multipath propagation and time variance in the case of a moving vehicle. We will see that the channel transfer function is time variant and random. The channel transfer function in the baseband is given by

$$H(f,t) = \sum_{l=0}^{P-1} e^{i\theta_l} e^{i2\pi f_{D_l} t} e^{-i2\pi f \tau_l} \tag{39}$$

where:

P: *Number of paths*
f_{D_l}: *Doppler shift for the l^{th} path*
τ_l: *Time delay of echo*
θ_l: *Phase shift*

The first exponent represents a random phase shift for the i^{th} path. The probability density function is given by [20]

$$p_{\theta_n}(\theta) = \frac{1}{2\pi}, \quad 0 \le \theta \le 2\pi \tag{40}$$

The second exponent represents the Doppler shift which depends on the direction of a received reflection with respect to the direction of the moving car.

Assuming that the angular distribution of wave arrival is uniformly distributed [20], the probability density function of the Doppler shift is

$$p_{D_t}(f) = D_{\max}\cos(\Phi)$$

$$\textit{where:} \qquad (41)$$

$$p_{\Phi}(\varphi) = \frac{1}{2\pi}, \quad 0 \le \varphi \le 2\pi$$

D_{max} is the maximum possible Doppler shift.

The third exponent represents the time delay of the echo. In a typical impulse response a grouping of time delays occurs around time delay values which are distributed with a greater difference (main reflections). These main reflections are specular reflections at objects far away from the receiving antenna. The spread of the main reflections is a result of scattering by objects near the receiving antenna. Figure 14 shows a multipath environment. There are three groups (main reflections). The local scattering is depicted by dotted lines.

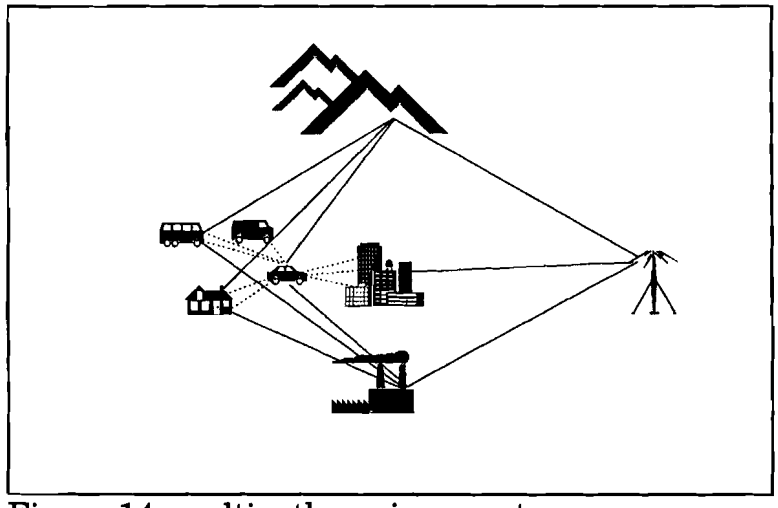

Figure 14. multipath environment.

The time delay density function representing a main reflection is approximated by an exponential distribution [6]:

$$p_{\tau_l}(\tau) = \frac{1}{T_m} e^{-\tau/T_m}$$

where: (42)

T_m: *standard deviation = delay spread*

Models have been developed describing delay profiles for rural, urban and hilly areas. In the program 6 models are implemented. Appendix G contains detailed information about the 6 profiles, which are implemented in the program.

The received signal r(t) as a function of the transmitted signal s(t) can be deduced from (24) as

$$r(t) = \sum_{l=0}^{P-1} e^{i\theta_l} e^{i2\pi f_{D_l} t} s(t-\tau_l) + noise \qquad (43)$$

For simulation simplification we assumed the random variables to be statistically independent.

4.3 Simulation results

4.3.1 Gaussian channel

The performance of the OFDM system in a **Gaussian** channel is independent of: the number of carriers, the number of active carriers, the use of frequency and time interleaving and the symbol duration time. The simulations are carried out without a guardband interval, since a guardband interval is useless in a Gaussian channel. The convolutional code which is used has an efficiency of 1/2 (2 code bits per data bit) and a constraint length K=7. The polynomial generators are 133 and 171.

The use of soft-decision decoding leads to a gain of approximately 2 dB compared with hard-decision decoding at relevant E_b/N_o values in a Gaussian

channel and it is easy to implement. Soft decision decoding requires more memory and memories are expensive. However, the system under test was provided with soft-decision decoding.

The simulation curves of the Gaussian channel are presented in Appendix E.

4.3.2 Rayleigh channel

The Rayleigh channel simulations are very time consuming on a PC. A simulation duration of one night is needed in order to calculate the BER for one E_b/N_o (on a 286 with coprocessor). A considerable amount of time could be gained by implementing the Rayleigh channel model on a DSP-board. This is particularly easy if the DSP-board supports the Pascal or C programming language. Another method saving simulation time, which has been implemented, is the following. The data at the output of the Rayleigh channel (without Gaussian noise) are saved on a hard disk during the simulation of the first E_b/N_o value. If more than one E_b/N_o is simulated, these data are read from hard disk and Gaussian noise with a proper variance (according to E_b/N_o) is added. The gain in speed by reading the data from hard disk is about five times compared with the simulation of the first E_b/N_o value.

Due to the long simulation time needed, it was not possible to do many experiments with the parameters. By using a more powerful PC it will be possible to experiment with for instance the time interleaving depth, different code rates, other frequency interleaving schemes, soft/hard-decision decoding etcetera. Another parameter of great interest is the bandwidth, since future generations of the DAB-system will use a smaller bandwidth.

The simulations showed that the performance does not depend heavily on the profile, because the duration of the impulse response did not exceed the guardband interval duration.

The simulation curves are presented in Appendix F. The parameters of the simulated system and the profile number (Appendix G contains the profile parameters) are given together with the plots. In the simulated system a mono audio channel consists of 8 symbols/frame. The DAB system under test uses 9 symbols per mono audio channel, but due to memory limitations of Turbo Pascal (time interleaving memory) this could not be implemented. However, the influence on the performance is supposed to be very low.

Appendices F.1 and F.2 contain the simulations for profile 1 (= rural) respectively with and without channel coding. Appendices F.3 and F.4 contain the simulations for profile 2 (= urban 1) respectively with and without coding.

5. Field trial

In this chapter important channel parameters will be presented. In order to analyze the system it is necessary to record the parameters, since it is impossible analyzing the large amount of data while driving around. A description of the methods used for acquiring and recording the parameters will be given. Finally the results of the mobile test drives will be presented.

5.1 Important parameters

There are three important parameters:
1. The channel impulse response
2. The channel transfer function
3. The channel BER

The **channel impulse response** gives information about the channel delay spread, which is important for a good choice of the guardband interval duration. The channel impulse response is calculated once in every 24 ms and depicts the response over the 7 MHz bandwidth. The channel impulse response and a synchronisation signal are available at the DAB-receiver. This signal can be monitored on an oscilloscope. In Appendix G the method used for the calculation of the impulse response is explained. The resolution obtained is about 0.125 µs.

The **spectrum** of the transmitted OFDM-signal is white. Consequently the spectrum of the received signal represents the channel transfer characteristics. Therefore we obtain the channel frequency response and an indication of the received signal strength by measuring the received signal spectrum.

The **channel BER** can be measured by re-encoding. This method is explained

in detail in Appendix H. Simulations have shown that this method is a reliable method for measuring in both a Gaussian channel and a Rayleigh channel a channel BER up to 10^{-1}. These simulation results are presented in Appendix H. This method is implemented in the Viterbi decoder chip which is used in the DAB-receiver. But it did not work. The data sheet stated that for error measurement the decoder system clock frequency must be at least 78 times higher than the decoder symbol clock frequency. But the data sheet contained an error. Consulting the manufacturer showed that instead of >78 it should be 76, 77 or 78. This condition is not met in the DAB-receiver. Therefore an extra circuit for measuring the channel BER in this manner has been built. The circuit diagram and a description is given in Appendix I.

A major advantage of this method for measuring the channel BER is the ability to do on-line channel bit error rate measurements.

5.2 Measurement setup

The three parameters mentioned above and the audio signal are the most significant. For the purpose of analysis it is important to record these data. A digital video recorder and a VHS recorder have been examined for this purpose. A major disadvantage which applies to both video recorders is the fact that TV synchronisation signals are necessary, otherwise they will not operate. Circumventing the need for synchronisation signals in a VHS recorder is perhaps theoretically possible, but since almost all functions are integrated in a single chip it becomes difficult. The digital video recorder consumes a lot of power (1200 Watt), which is not very suitable in a mobile environment. Besides, the digital video recorder is not always available.

The option finally considered (and also chosen) is an instrumentation recorder. The instrumentation recorder used was a (10 year old) Racal Store 4DS recorder. There are four data channels available. The maximum available

bandwidth is two FM data channels 0-20 kHz and two direct recording (D.R.) data channels 100 Hz - 300 kHz. This applies for the maximum tape speed (60 inch/s). Since one FM channel dit not operate well, the maximum usable tape speed was 30 inch/s. The available bandwidth now becomes: 2 FM channels 0-10 kHz and two D.R. channels 100 Hz - 150 kHz.

The **impulse response** (except the synchronisation signal) can be recorded on one FM channel. 10 kHz bandwidth is sufficient.
The resolution of the impulse response, which is calculated by the DAB-receiver, is 0.125 µs. The DAB-receiver is not capable of detecting and visualising an impulse response spread which is larger than the symbol duration = 80 µs.

The **spectrum** of the received signal occupies 7 MHz bandwidth. It is possible to convert the received signal to baseband and record the baseband signal. For analysis this baseband signal could then be monitored with a spectrum analyzer. But this method can only be used if 7 MHz baseband bandwidth is available on the recorder. However, by using a clever trick it is possible to record the spectrum on one FM channel (10 kHz bandwidth !) by making a record of the picture information of the spectrum analyzer : take a spectrum analyzer with a video output (HP 8558B) and record this signal. The video output can be monitored with an oscilloscope and the oscilloscope picture is the same as the picture on the screen of the spectrum analyzer. The spectrum analyzer delivers a synchronisation signal which is used for the triggering of the oscilloscope.
The spectrum of the received signal is used in order to determine the power of the received signal (in dBm). This is done by hand. The accuracy is affected if the spectrum is non-white. The accuracy is estimated at ± 5 dBm.

The **channel BER** measurement equipment produces two signals. The first signal is the clock signal of the decoded data. This clock is identical to the

Viterbi decoder symbol clock. The clock and therefore the data are decoded in burst mode: the clock is active during 16.128 ms of a 24 ms frame and the burst clock frequency is 250 kHz. The average datarate is 168 kbit/s (one mono channel). The second signal is the error signal. The error signal output is high when an error is detected. In this case the output remains high for the duration of a half clock period. The error signal output operates in burstmode too.
If both signals are connected to a counter which calculates the ratio between the error signal frequency and the clock frequency, then the channel BER is calculated. Only the error signal needs to be recorded, because if we play back the recordings we can generate an artificial clock with a 168 kHz pulse generator.
This artificial clock is not a burst clock, but if the counter bases the BER calculation on a period (sample period) which is sufficiently longer (10 times) than 24 ms, we get virtually the same result. The sample period is ± 400 ms. This corresponds to approximately 17 frames. The error is in this case less than 2%. The lowest BER which is measurable by the counter, if the sample period is 400 ms, is 10^{-5}.
The bandwidth available for recording the error signal is 150 kHz. This is not enough to record accurately sequential error pulses. If two or more errors occur sequentially only one error pulse can be detected. However the error introduced by this phenomenon can be neglected for low bit error rates ($<10^{-2}$) and for a BER of 10^{-1} (limit of operation for audio decoder) a test showed that the deviation is less than 5%.
The total accuracy is therefore approximately 7%.

Finally we want to record the **audio signal**. For this purpose only a mono audio signal needs to be recorded. Earlier test drives have shown that both audio channels perform equally. The only channel available is a D.R. channel. The low frequency response of a D.R. channel is not very good, but for an appropriate recording of the impulse response and the spectrum a good low frequency response is essential and only two FM channels were available.

Therefore the audio signal was recorded on a D.R. channel and not on a FM channel.

One problem remains: there are 4 data channels available on the instrumentation recorder and we have 6 signals, namely the four mentioned above and two synchronisation signals. But fortunately there is bandwidth available, since the audio signal occupies only 20 kHz. So the frequency range 20 kHz - 150 kHz is still available. A modem has been built to modulate and demodulate the synchronisation signals by using two carriers on the frequencies 111.86 kHz and 138.55 kHz. The circuit diagram and a description of the modem is given in Appendix J.

In figure 15 a diagram of the measurement configuration is given.

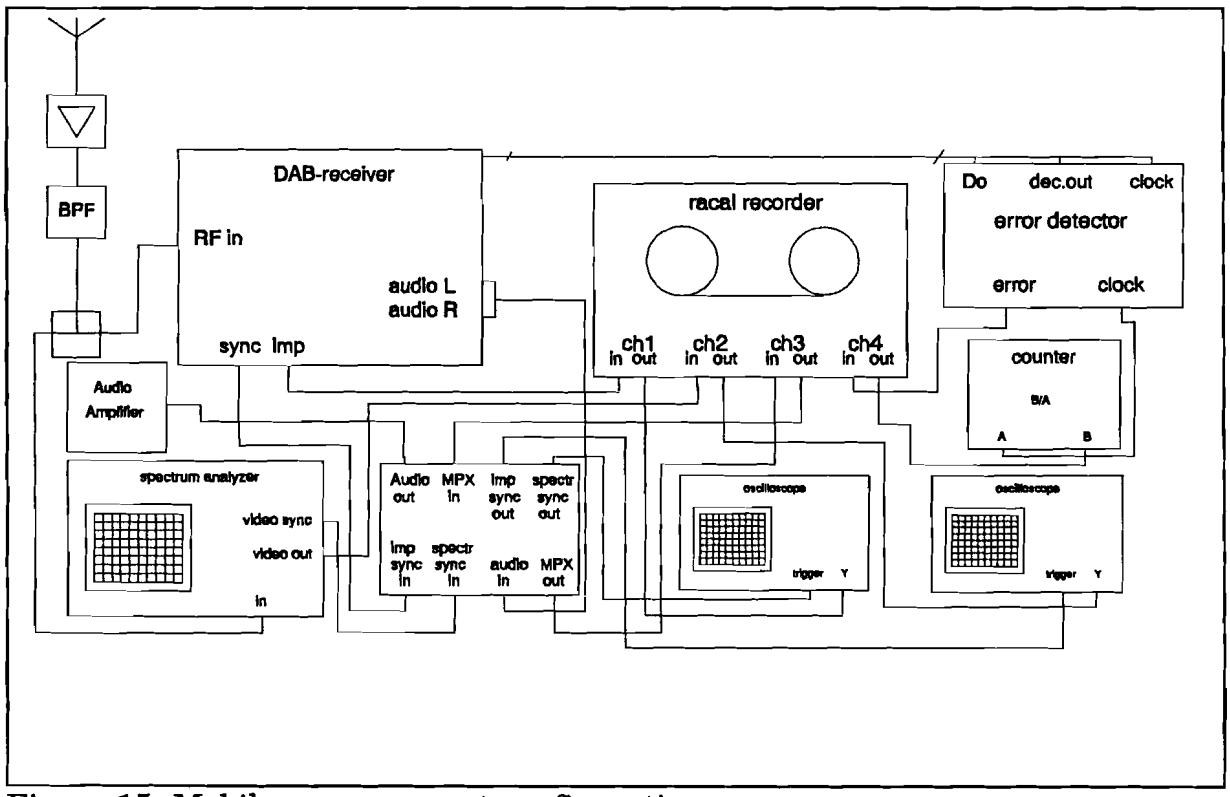

Figure 15. Mobile measurement configuration.

The setup used for the analysis of the recorded data is given in figure 16.

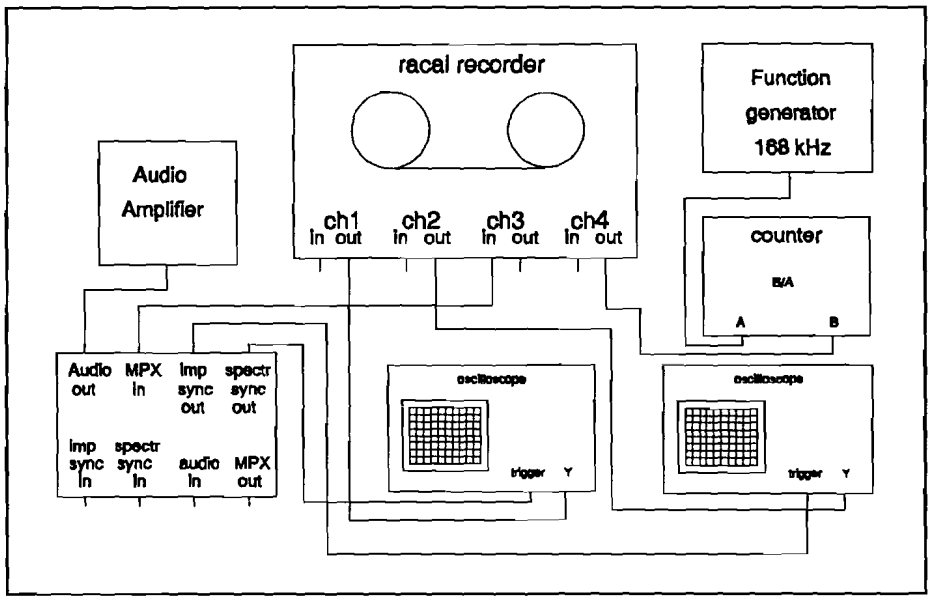

Figure 16. Analysis of recorded data.

5.3 Measurement results

5.3.1 Subjective results

The COFDM/MUSICAM system proved to be very robust against multipath propagation. The digital nature of the system is reflected in the audio quality: the audio quality was perfect whenever the received field strength was above a certain threshold level. Below a certain level there was no audio recognizable (the mute did not work perfectly during the test drives: when the decoder failed strange sounds where produced). In the transition range a gurgling sound was produced, however the transition is sharp.

The reception of multiple reflections did not cause the system to fail. If the shape of the received spectrum deviated strongly from a rectangular shape, the system continued to provide service.

The gap-filler was very effective in a badly served area in the vicinity of the university. Without the use of the gap-filler the reception was stammering and with the use of the gap-filler the reception was perfect. The transition from main transmitter to gap-filler as the dominating signal and vice-versa did not cause audible effects.

5.3.2 Objective results

A number of plots of the spectrum of the received signal and the impulse response have been made. The next two plots are used as an introduction.

In figure 17 a plot of a non-white spectrum of the received RF-signal is given. 1 division along the X-axis represents 1 MHz.

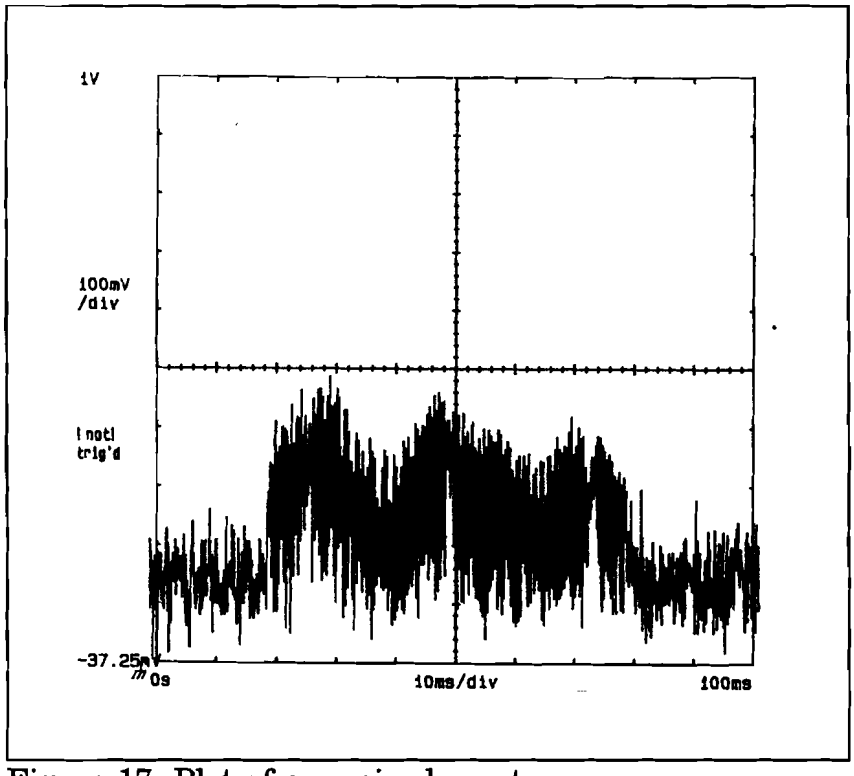

Figure 17. Plot of a received spectrum.

The spectrum is used in order to estimate the power of the received signal. The received (and recorded) spectrum has been calibrated by measuring the spectrum of an OFDM test signal with a known power, namely -3 dBm at the

output of an OFDM transmitter at 762 MHz. The spectrum is recorded by using a dB scale on the spectrum analyzer. A resolution bandwidth of 30 kHz has been used. If the spectrum of the received signal (7 MHz bandwidth) is white, then 0 Volt on the oscilloscope represents a received signal strength of -100 dBm and 0.8 Volt represents -20 dBm. A problem is the internal noise of the spectrum analyzer: If no input signal is connected, there is white noise present. The level of this noise is 0.2 Volt on the oscilloscope. A consequence is that received signal strengths <-80 dBm (having a white spectrum) are not detectable. The sensitivity of the DAB-receiver is -92 dBm. However, the spectrum analyzer used was the only one available which combined a low power consumption and a video output. A great disadvantage of the spectrum analyzer is frequency instability. The spectrum analyzer needs a warm up of one hour in order to be stable. The instability of the spectrum analyzer is the reason why the recordings may show sometimes a spectrum which is not correctly centred.

Figure 18 shows an impulse response. One division (1 ms) represents about 4 µs. The exact number is 1 ms/256 = 3.9 µs. The impulse response is calculated once in every 24 ms and a scaling of the time base is convenient when displaying the impulse response on an oscilloscope. The plot shows that

the first reflection is not always the strongest reflection.

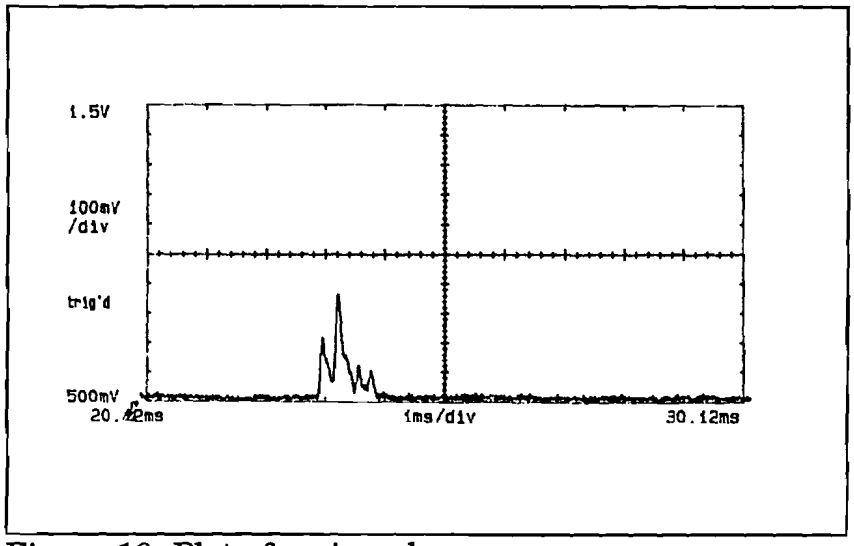

Figure 18. Plot of an impulse response.

The next plot (figure 19) shows an impulse response with the gap-filler turned on.

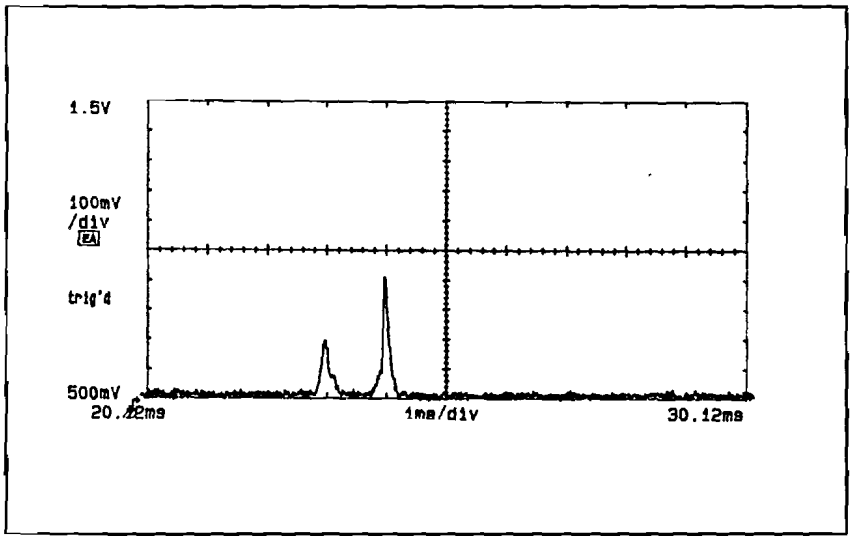

Figure 19. Gap-filler internal delay.

The impulse response is recorded in a street called the Amazonelaan. This street is a continuation of the line Natlab - University. Therefore the delay between the two pulses represents the internal delay of the gap-filler. The gap-filler delay is thus approximately 4 µs. Another way to measure the delay of the gap-filler is examining the impulse response at a point close to the gap-filler. This yields the same result.

Very interesting is the alteration of the impulse response in the transition region between main transmitter and gap-filler. The following series of plots are recorded in a street called Loondersmolen. The gap-filler transmit antenna has been directed to this street during the tests described below. The gap-filler location is in line with this street. The first plot (figure 20) is at the beginning of the street. At this point the gap-filler is directly visible.

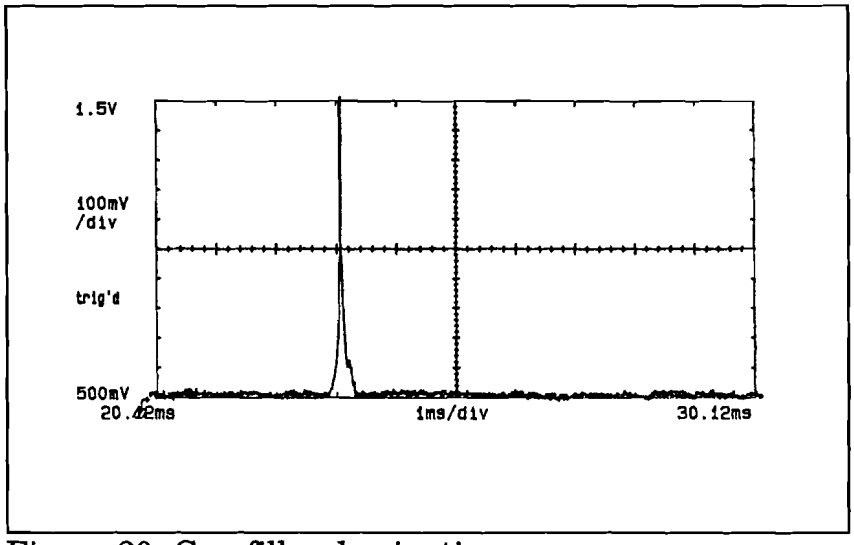

Figure 20. Gap-filler domination.

We see one strong impulse. Driving in the direction of the gap-filler causes shadowing, caused by a flat at the end of the street. The next plot (figure 21) shows a weaker impulse from the gap-filler than the impulse of the main

transmitter.

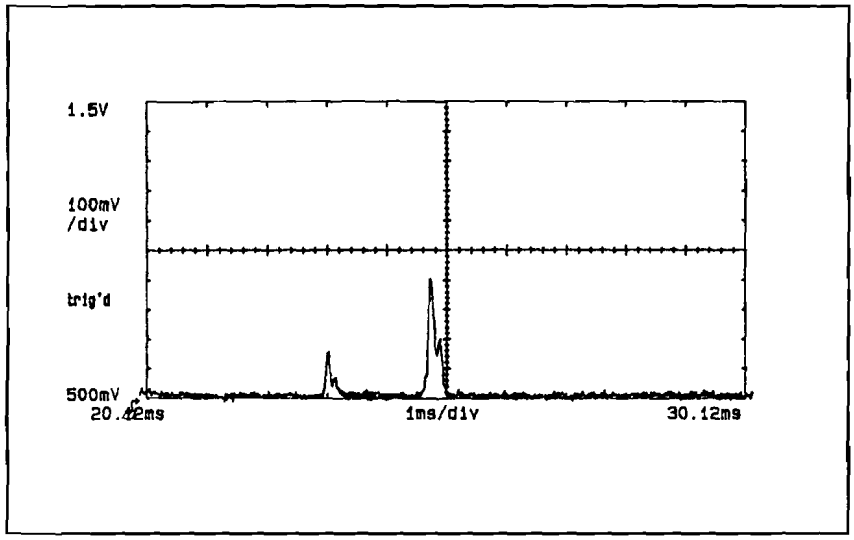

Figure 21. Gap-filler less dominating.

At this point the gap-filler is not directly visible. Driving further in the direction of the flat mentioned above causes more shadowing and both impulses become equally strong (figure 22).

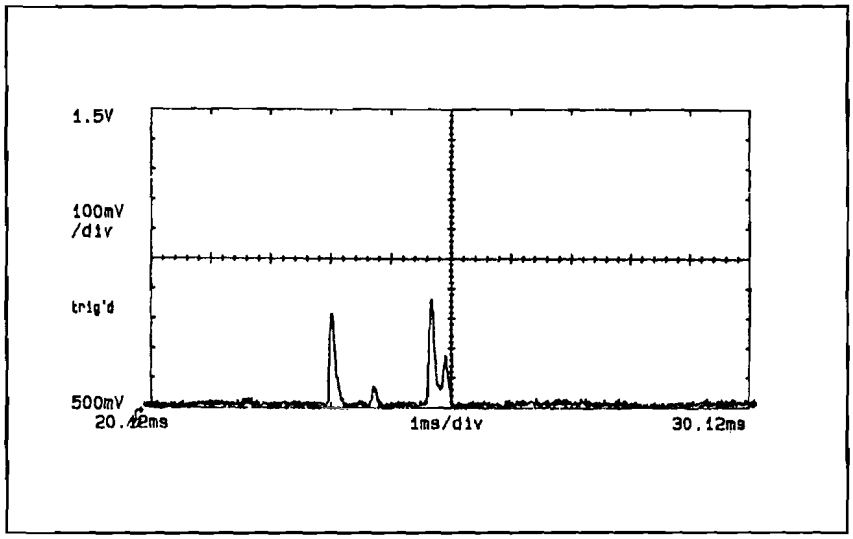

Figure 22. Both impulses equally strong.

The transition occurred without any noticeable effect on the audio quality. The BER is only dependent of the signal strength and independent of the echo situation.

The system can handle even larger delay spreads. This is shown in the next

plots: figure 23 with the gap-filler turned off and figure 24 with the gap-filler turned on at approximately the same location.

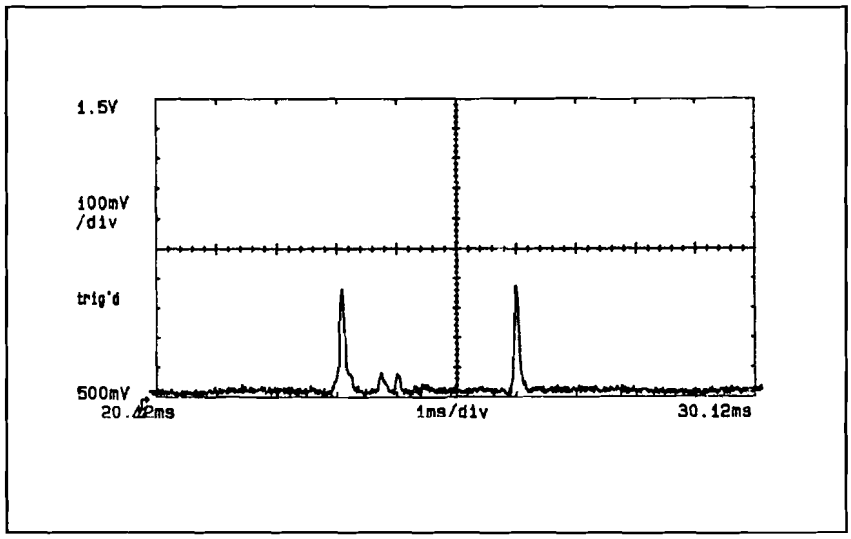

Figure 23. Large delay spread, gap-filler off.

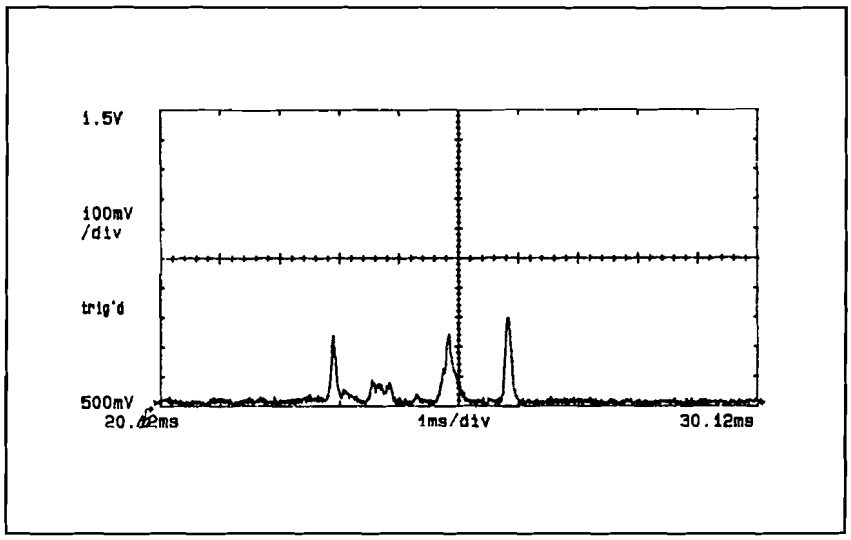

Figure 24. Large delay spread, gap-filler on.

The delay between the first and last echo is 12 µs. The audio quality is still perfect.

A very interesting event occurred in a street called Stevertse Molen. The gap-filler was turned on. A impulse response which is recorded in this street is

given in figure 25.

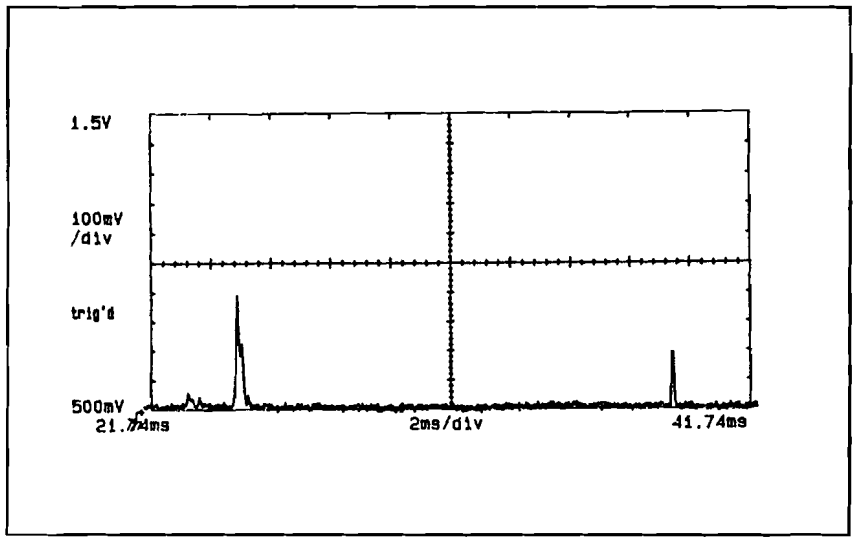

Figure 25. Reflections from gap-filler.

The X-axis scale is now 8 µs/division. We see a strong reflection, which is a direct impulse from the gap-filler. Before this impulse there is a weak impulse visible from the main transmitter. The last echo is situated 60 µs after the first echo. This echo is an echo from the gap-filler, because this echo was not present when the gap-filler was turned off. The delay exceeds the guardband duration and this was clearly seen in the BER: the BER increased from $<10^{-3}$ to $2 \cdot 10^{-2}$ although the received signal strength was roughly the same. The audio was not affected, because the BER remained smaller than 10^{-1}. The delay time is very long, since 60 µs corresponds to 18 km. However, the third impulse is very strong, in spite of the fact that 18 km corresponds to approximately 19 dB additional free space loss at a distance of 0.5 km from the gap-filler. It could be that the impulse response calculation of the DAB-receiver was erroneous, however the BER was seriously affected.

The gap-filler is capable of enhancing the field strength in the service area of the gap-filler. This is shown in the next two plots. Figure 26 shows the received spectrum in the Loondersmolen without the gap-filler. There is practically no field present.

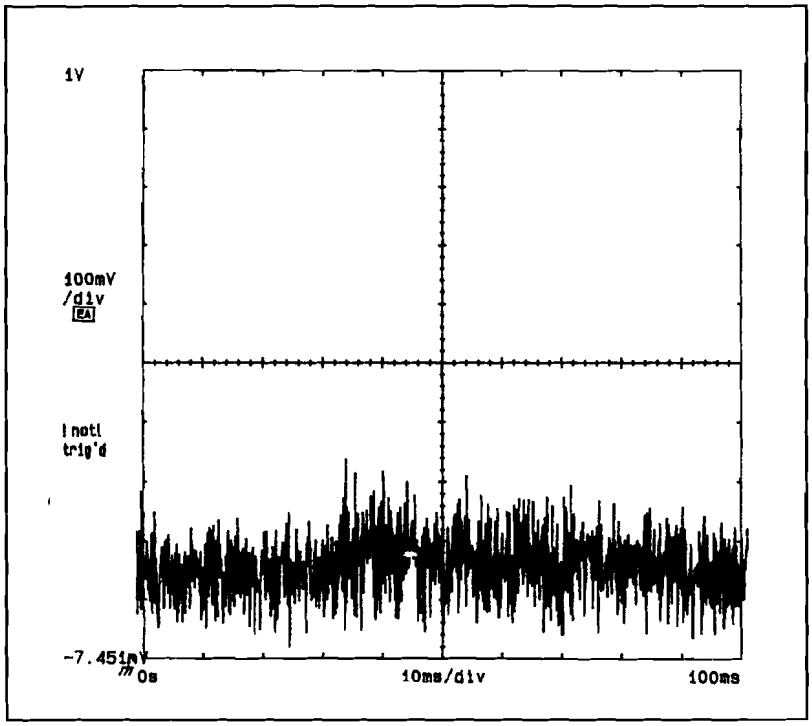

Figure 26. Received spectrum, gap-filler off.

Figure 27 shows the received spectrum at the same location with gap-filler on.

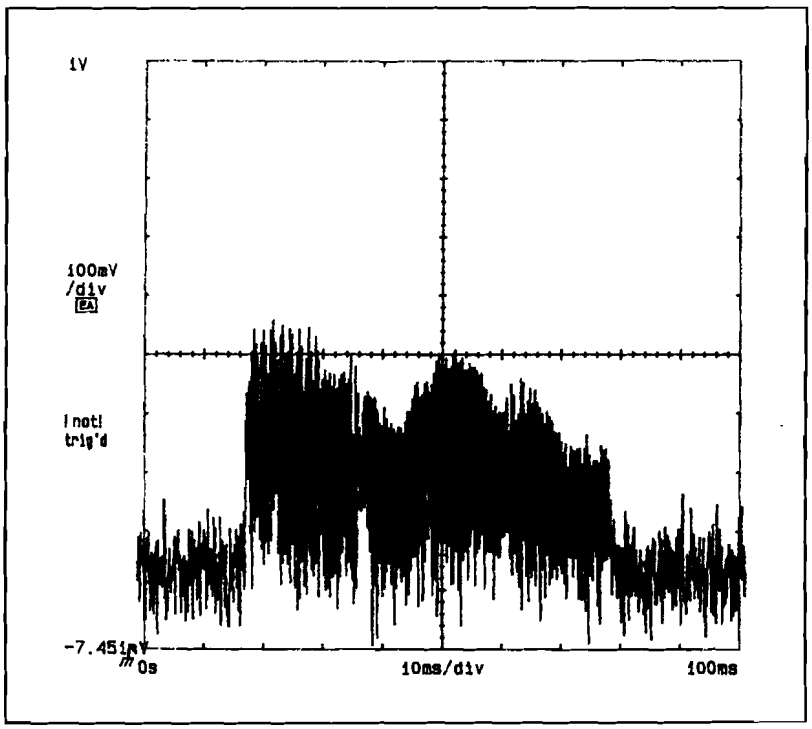

Figure 27. Received spectrum, gap-filler on.

These two plots illustrate the corresponding audio quality observed: with the gap-filler turned off the audio was stuttering, because the power of the received signal was near the threshold level of -92 dBm. With the gap-filler turned on the audio quality was perfect.

The system never failed when the received signal strength was above -80 dBm. In the case of a system failure there was no received signal spectrum visible. The performance of the system showed to be solely dependent on the received signal power and independent of the shape of the impulse response, because the duration of the impulse response is less than the duration of the guardband interval.

When the channel BER exceeded 10^{-1} the system did not provide service. The BER at the output of the Viterbi decoder is then, according to the Rayleigh channel simulation results, between 10^{-3} and 10^{-2}. An exact number can not be given, since a small change in the channel BER corresponds to a large change in the BER after the decoder. Besides, the relation between the BER at the input of the decoder and the BER at the output of the decoder depends on the channel properties. If the channel BER is lower than approximately $7x10^{-2}$ the audio quality is perfect. In the transition region a gurgling sound is produced, but the audio remains recognizable.

A detailed analysis of the coverage area has not been made, since the frequency which will be used for the consumer version of the DAB-system will probably be much lower. The propagation characteristics are frequency dependent. Like the Okumura model predicted, the percentage of the locations at the edge of the service area covered by the main transmitter (7 km) and the gap-filler (3 km), is far beneath 100%. This is the reason why the gap-filler only is 100% effective at a distance lower than 3 km from the gap-filler.

6 Recommendations for future work

In this chapter some suggestions for future measurements will be given. The information which can be generated by the DAB-receiver will be described and some advice for field work will be given.

The **impulse response**, which is calculated by the DAB-receiver, has proven to be a very useful characteristic to measure. The calculation of the impulse response is not difficult to implement, so this should not be omitted in test receivers of future generations.
It would be very helpful if the impulse response signal would be available in a digital representation. This is convenient for determining statistics of the impulse response (for instance the spread) by processing the data with a PC.

The method used for measuring the channel **BER** has been described already. Due to an error in the datasheets of the Viterbi decoder channel BER measurement did not work. Of course this should be working correctly in future test receivers.
An additional mono audio channel would be convenient for measuring the BER *after* the decoder.

Displaying the **received spectrum** is very useful, since it contains information about the channel frequency response and the received signal strength. A method for recording the spectrum using a bandwidth which is much less than the bandwidth of the signal itself, has been described in chapter 5. This saves a lot of costs, since an 8 MHz digital instrumentation recorder is not cheap.

Measuring the **received signal strength** is difficult, since the signal bandwidth is much wider than most measuring receivers and simple power meters are not sufficiently sensitive. A method, which is worth trying, is this:

use a digital oscilloscope for displaying the spectrum (video out of the spectrum analyzer, chapter 5) and use an oscilloscope which is able to calculate the area of the displayed signal. A problem could be the speed of the oscilloscope, since in a mobile channel the variations occur fast. Perhaps there are spectrum analyzers available which are able to do this calculation by themselves.

A better (digital) **instrumentation recorder** would be very convenient. The audio was very poor in quality and mono, but this is not very important in this case. Tape jitter had a negative influence on the display of the impulse response. It was not a pleasure to watch the impulse response. The limited number of data channels caused some troubles recording all the signals. A modem had to be built. More data channels would be very helpful.

The addition of a mobile channel model in the COFDM simulation program makes it possible to analyze a number of aspects which have not been studied yet, like:

- the effect of reducing the OFDM transmission bandwidth
- the effect of non-uniform quantizing in case of soft decision decoding
- the effect of the number of soft decision bits

7 Conclusions

The simulations have shown that the COFDM modulation technique is able to overcome the problems encountered in a mobile radio channel, namely multipath propagation and fading.

The COFDM system is a digital transmission system, which is capable to cope with the problems encountered in a mobile radio channel. The service area is solely determined by the field strength, provided that the duration of the impulse response is smaller than the guardband interval duration. Under this condition the performance is independent of the shape of the impulse response and frequency response of the channel.

A co-channel relay (gap-filler) is able to enhance the reception quality in a badly served area. The gap-filler signal is from the point of view of the receiver merely an additional reflection. Thus, if the duration of the impulse response of the total system, main transmitter and gap-filler, is smaller than the guardband interval duration, then the performance of the total system is only dependent on the field strength. The transition from main transmitter to gap-filler and vice-versa occurs smoothly without any audible effects.

The duration of the impulse response did not exceed 12 µs during the test drives. However, a guard interval duration of 16 µs may be too low if more powerful transmitters are used, which is the case if a network is designed covering a whole country, particularly in case of a single frequency network. In this case larger differences in distances between several propagation paths are expected.

The reception reliability should be considerably better. If only 50% of the locations at the edge of the service area are covered, it is not acceptable,

because the service is then completely interrupted at 50% of the locations at the edge of the service area.

References

[1] Wozencraft J.M., Jacobs, I.M.
Principles of communication engineering.
New York, Wiley, 1965.

[2] Alard, M., Lasalle, R.
Principles of modulation and channel coding for digital broadcasting for mobile receivers.
EBU Rev. Tech., No. 224, August 1987, p. 168-90.

[3] Dosch, C., Ratliff, P.A., Pommier, D.
First public demonstrations of COFDM/MASCAM. A milestone for the future of radio broadcasting.
EBU Rev. Tech. (Belgium), 1988, No. 232, p. 275-83.

[4] Shelswell, P., Bell, C.P., Stott, J.H., Wakeling, S.,
Maddocks, M.C.D., Moore, J.H., Durrant, P.D. and Rudd, R.F.,
Digital Audio Broadcasting: The first UK field trials.
BBC Research Department Report 1991/2.

[5] Maddocks, M.C.D.
DAB: results of coverage area surveys using different COFDM bandwidth and transmit frequencies.
BBC Research Department Technical Memorandum No. T-1040.

[6] Le Floch, B., Halbert-Lasalle, R., Castelain D.
Digital sound broadcasting to mobile receivers.
IEEE Trans. Consum. Electron., Vol. 35(1989),
No. 3, p. 493-503.

[7] 1st World Electronic Media Symposium. Speakers Papers. Technical Symposium. New Horizons in Electronic Mailing. Ratliff,P.A.
EBU/DAB studies for a new digital sound radio broadcasting system - CD quality for mobiles.
Geneva, 4th to 7th Oct. 1989, ITU, 1989, p. 377-84.

[8] 1st World Electronic Media Symposium. Speakers Papers. Technical Symposium. New Horizons in Electronic Mailing. Dehery, Y.F.
A digital audio broadcasting system for mobile reception.
Geneva, 4th to 7th Oct. 1989, ITU, 1989, p. 53-7.

[9] EUROCON 88: 8th Conference on Electrotechnics. Conference Proceedings on Area Communication.
Halbert, R. Le Floch, B., Pommier, D.
A new system of sound broadcasting to mobile receivers.
Stockholm, 13-17 June 1988, New York, IEEE, 1988.

[10] Pommier, D., Ratliff, P.A.
New prospects for high-quality satellite sound broadcasting to mobile, portable and fixed radio receivers.
Brighton, 23-27 september 1988, Norwich, IEE, 1988.

[11] Cimini, L.J.
Analysis and simulation of a digital mobile channel using orthogonal frequency division multiplexing.
IEEE Transactions on Communications, Vol. COM-33(1985), No. 7, p. 665-675.

[12] Turin, G.L.
Introduction to spread spectrum antimultipath techniques and their application to urban digital radio.
Proc. IEEE, Vol. 68(1980), No. 3, p. 328-353.

[13] Pommier, D., Wu Yi.
Interleaving or spectrum spreading in digital radio intended for vehicles.
EBU Review, No. 217, June 1986, p. 128-142.

[14] Zogg, A.
Multipath delay spread in a hilly region at 210 MHz.
IEEE Transactions on Vehicular Technology, Vol. VT-36(1987), No.4, p. 184-187.

[15] Böer, A.
Power Transfer in Multipath Channels.
Institut für Rundfunktechnik, Feb. 91
(preliminary english version).

[17] GLOBECOM '89. IEEE Global Telecommunications Conference and Exhibition. Communications technology for the 1990s and Beyond.
Rault, J.C., Castelain, D., Le Floch, B.L.
The coded orthogonal frequency division multiplexing (COFDM) technique, and its application to digital radio broadcasting towards mobile receivers.
Dallas, 27th to 30est November 1989, Vol. 1, IEEE, New York, 1989.

[18] Plaats, J.C. van der.
Digital Audio Broadcasting (Eureka 147) : Orthogonal Frequency Division Multiplexing (OFDM) : Quaternary Phase Shift Keying (QPSK) with Guardband Interval Modulation for Digital Audio Broadcasting (DAB).
Graduation report Eindhoven University of Technology, Faculty of Electrical Engineering.
Eindhoven, 1989, report No. 5536.

[19] Jakes, W.C.
Microwave mobile communications.
New york, John Wiley, 1974.

[20] Lee, W.C.Y.
Mobile communications engineering.
Mac Graw Hill, 1982.

[21] Okumura, Y., Ohmori, E., Kawano, T., Fukuda, K.
Field strength and its Variability in VHF and UHF land-mobile services.
Review of the Electrical Communication Laboratory,
Vol. 16, Nos. 9-10, September-October, 1968.

Appendix A: Datasheet power splitter

KATHREIN

Medium Power Splitters

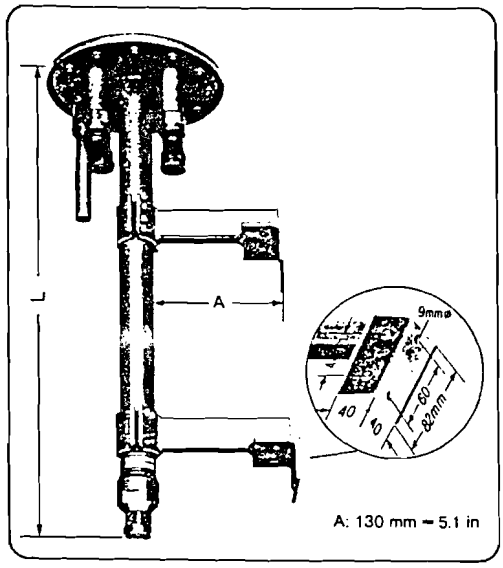

Medium power splitters for connecting several antennas

Frequency range	Band I: 47 ... 88 MHz	FM: 87.5 - 108 MHz	Band III: 174 - 230 MHz	UHF: 470 - 790 (860) MHz
Input power	3 kW	2.5 kW	2 kW	1kW
Impedance	50 Ω			
Number of outputs	2 to 8			
RF-connections	7/16 female			
Tuning	These splitters are also available with tuning device			
SWR	< 1.05 in each frequency range resp. in the operating channel			
Insertion loss	< 0.05 dB			
Special models	The splitters are also available with different power splitting			
Typical design	Coaxial line transformer (see fig.)			
Pressurization	The splitter can be provided with dry air after simple mounting of a sealing screw (supplied). Typical operating pressure: 300 hPa (300 mbar)			
Weather protection	The RF-connectors may be protected by means of supplied sealing straps			
Material	Outer conductor: Brass, lacquered in grey RAL 7032, inner conductor: Aluminum			
Mounting	To flat planes by means of supplied standard mounting brackets, or to tubes with 30 - 340 mm diameter using 2 pcs of additional tension bands No. 759 044, separate order. Also see mounting hardware page 98			

*) further splitters on request

Type No. of some splitters with equal power splitting*)

Frequency range MHz	for connecting of ... antennas	Typical length L mm (in)	Type No.
47-54	2	3050 (120)	K 62 55 8 1 A
	3		K 62 56 8 1 A
	4		K 62 57 8 1 A
	5		K 62 58 8 1 A
	6		K 62 59 8 1 A
54-61	2	2700 (106.3)	K 62 55 8 2 A
	3		K 62 56 8 2 A
	4		K 62 57 8 2 A
	5		K 62 58 8 2 A
	6		K 62 59 8 2 A
61-86	2	2400 (94.5)	K 62 55 8 3 A
	3		K 62 56 8 3 A
	4		K 62 57 8 3 A
	5		K 62 58 8 3 A
	6		K 62 59 8 3 A
87.5-108	2	1650 (65)	K 62 55 1 A
	3		K 62 56 1 A
	4		K 62 57 1 A
	5		K 62 58 1 A
	6		K 62 59 1 A
174-230	2	1200 (47.2)	K 62 55 5 A
	3		K 62 56 5 A
	4		K 62 57 5 A
	5		K 62 58 5 A
	6		K 62 59 5 A
470-860	2	550 (21.6)	K 63 55 4 A
	3		K 63 56 4 A
	4		K 63 57 4 A
	5		K 63 58 4 A
	6		K 63 59 4 A

Tunable Splitters
(tunable to a single channel)

174-230	2	900 (35.4)	K 62 60 5 A
	3		K 62 61 5 A
	4		K 62 62 5 A
	5		K 62 63 5 A
	6		K 62 64 5 A
470-860	2	700 (27.6)	K 63 60 4 A
	3		K 63 61 4 A
	4		K 63 62 4 A
	5		K 63 63 4 A
	6		K 63 64 4 A

Appendix B: Datasheets main transmitter antenna

B.1 General datasheet

KATHREIN | **Directional Antenna K 72 31 4 . ., K 73 31 4 . .**
470 - 790 (860) MHz

Horizontally or vertically polarized broadband aluminum panel in fibreglass radome

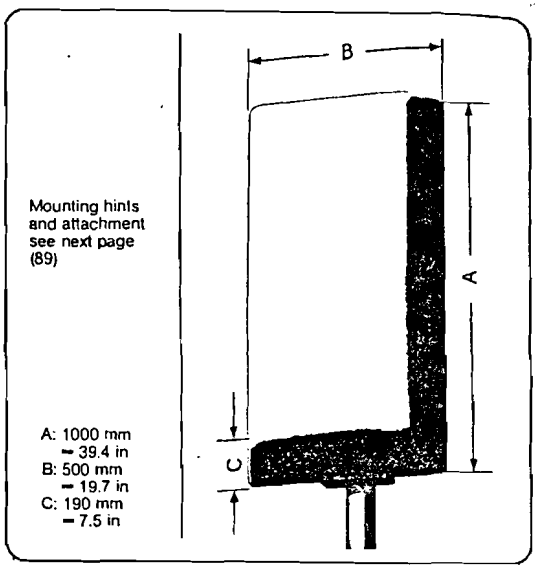

Dipole arrangement	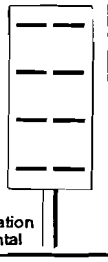 Polarization Horizontal	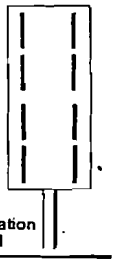 Polarization Vertical
Type No.	K 72 31 4 1 K 72 31 4 7 715 022	K 73 31 4 1 K 73 31 4 7 757 627
Input	N female 7/16 female 13/30 female	N female 7/16 female 13/30 female
Polarization	Horizontal	Vertical
VSWR	< 1.1	< 1.12
Frequency range	470 - 860 MHz	470 - 790 (860) MHz
Gain	11 dB (ref. to λ/2-dipole)	
Max. power	N female: 0.5 kW, 7/16 female: 1 kW, 13/30 female: 2 kW (higher power on request)	
nbinations	The antenna is especially suitable as a component in arrays to achieve various radiation patterns	
Scope of supply	Antenna with two types of weather protective housings for the connector	
Material	Dipoles and reflector screen: weatherproof aluminum. Radome: Fibreglass. Fittings: Hot-dip galvanized steel	
Radome colour	Standard: White (RAL 9002); upon request available in red (RAL 2002) or grey (RAL 7001)	
Mounting (order separately)	By means of clamps K 61 14 0 . . to pipes of 40 . . . 521 mm ∅ = 1⁹/₁₆ . . . 20 ½ in (see page 89)	
Ice protection	Since the radiators are fully protected by the radome and due to its very sturdy construction, this antenna will remain operational even during heavy icing	
Grounding	Grounding via mounting parts	

Mechanical data

Wind load (at 1[illegible] m/h = 100 [illegible]	frontal: 815 N = 180 lbs lateral: 250 N = 55 lbs
Max. wind velocity	225 km/h = 140 mph
Weight	12 kg = 26.5 lbs
Packing	106 x 50 x 25 cm = 42 x 20 x 10 in

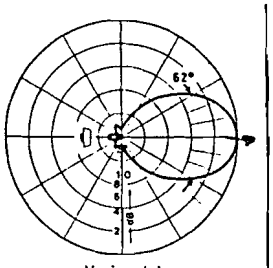

Horizontal

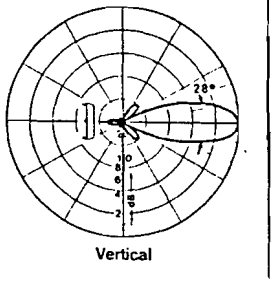

Vertical

Radiation pattern
(at mid-band)

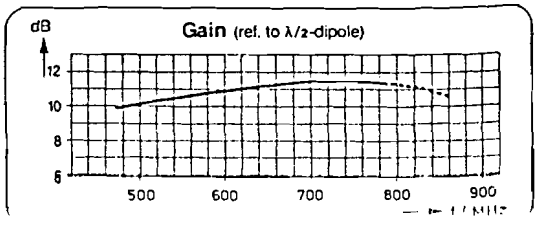

B.2 Horizontal radiation pattern (valid for one antenna and array)

KATHREIN WERK 2 PTR 802

Frequenz (MHz): 770
Datenfile Nr. : 46

Azimut (Grad)	Abstand (mm)	Versatz(+;-mm)	Phase (Grad)	Leistung(-fach)
90.0	0	0	0.0	1.00

G_{max}/G_{mittel} (dB): 7.98

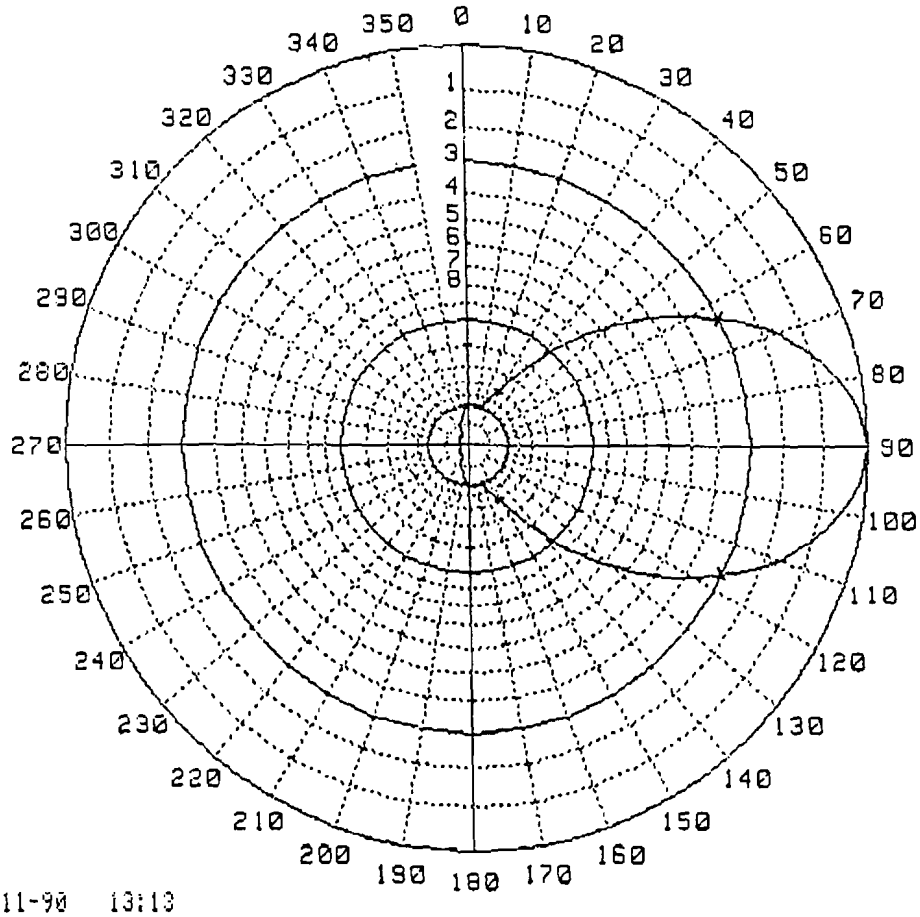

06-11-90 13:13

Horizontaldiagramm eines Antennenfeldes K733147

KATHREIN D-8200 ROSENHEIM	UHF - Sendeantenne	Typ Nr.
PTR Obereder	Kanal 57 - 60	Bl. 101

B.3 Vertical radiation pattern antenna array

KATHREIN WERK 2 PTR 803

Frequenz (MHz): 770
Datenfile Nr. : 616

Nr.	Abstand (mm)	Vorversatz(mm)	Phase (Grad)	Leistung(-fach)
2	1120	0	0.0	1.00
1		0	0.0	1.00

E-Faktor: 1.00

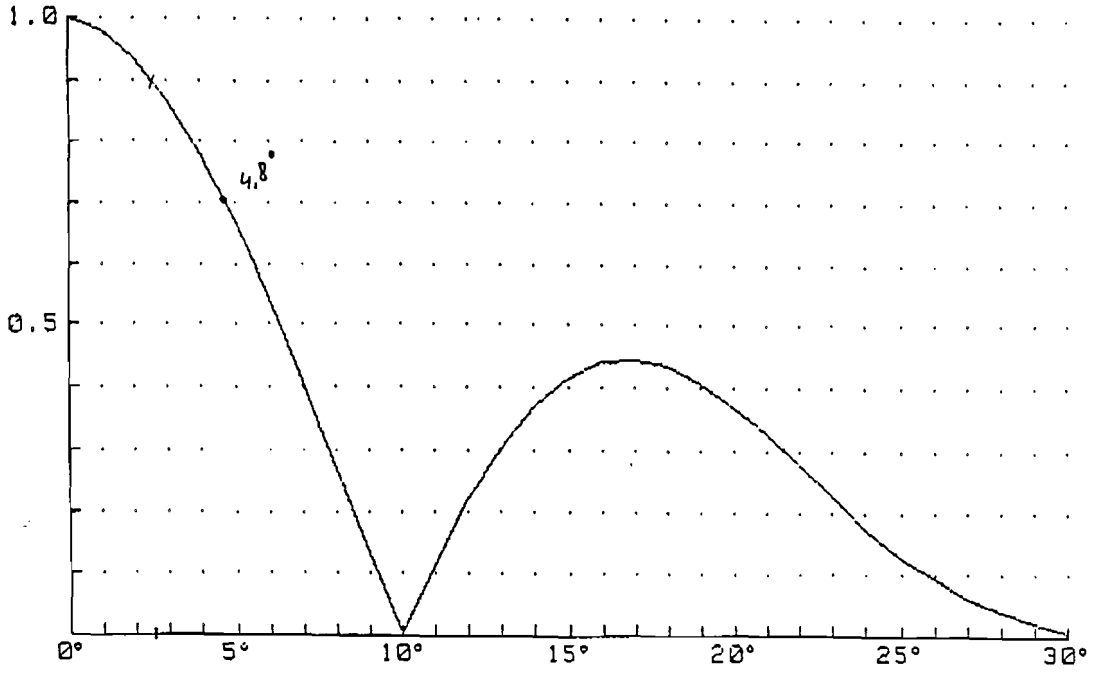

06-11-90 13:07

2 Antennenfelder K733147 übereinander

KATHREIN D-8200 ROSENHEIM	UHF - Sendeantenne Kanal 57 - 60	Typ Nr.
PTR Obereder		Bl. 102

Appendix C: Coverage area main transmitter (-3 dB)

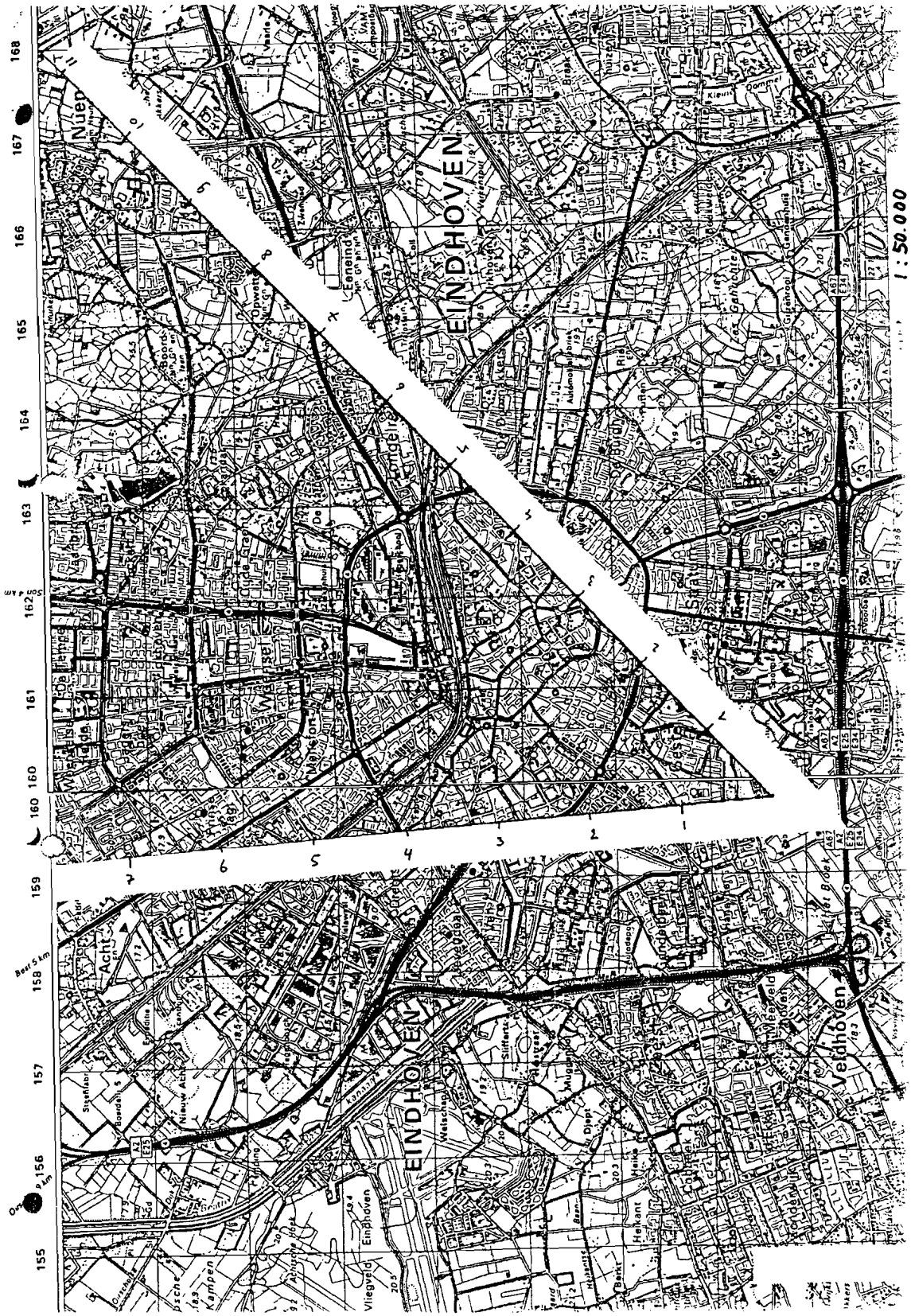

Appendix D: Datasheet gap-filler antenna

KATHREIN

Directional Antenna K 72 23 4 . .
470 - 860 MHz

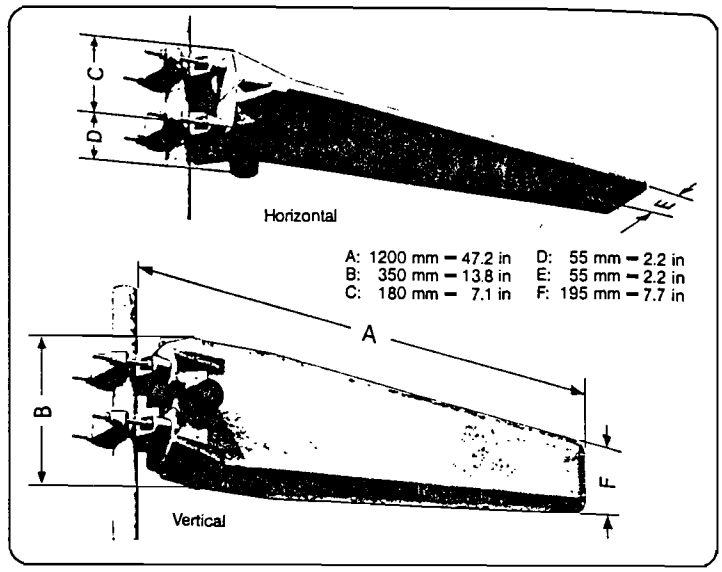

Logarithmic-periodic broadband directional antenna in fibreglass-radome.
High side-lobe suppression

Type No.	K 72 23 4 7	K 72 23 4 1
Imput	7/16 female	N female
Impedance	50 Ω	
Frequency range	470 - 860 MHz	
Gain	9 dB (ref. to λ/2-dipole)	
VSWR	< 1.25	
Side-lobe suppression	> 23 dB (500 - 800 MHz: > 25 dB)	
Polarization	Horizontal or vertical by conversion of the clamps	
Max. power	30 Watts (higher power on request)	
Combinations	Two or more antennas may be connected to attain higher gain and radiation patterns with very high side-lobe suppression	
Material	Weatherproof aluminum. Radome: fibreglass	
Mounting	To pipes of 48-115 mm = 1⅞-4½ in dia. by means of mounting clamps, supplied	
Ice protection	Since the radiators are fully protected by the radome and due to its very sturdy construction, this antenna will remain operational even during heavy icing	
Grounding	Grounding via mounting parts	

Mechanical data

Wind load 160 km/h = 100 mph Horizontal Vertical	frontal/lateral: 63/102 N = 13.9/22.5 lbs frontal/lateral: 63/500 N = 13.9/110 lbs
Max. wind veloc. Horizontal/Vertic.	220 km/h/180 km/h = 140 mph/112 mph
Weight	9 kg = 19.8 lbs
Packing	117 x 37 x 19 cm = 46 x 15 x 7.5 in

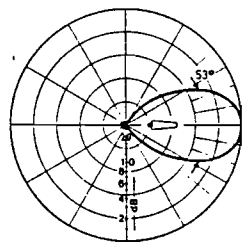

in E-plane

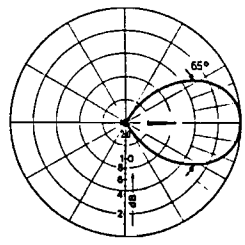

in H-plane

Radiation pattern
(at mid-band)

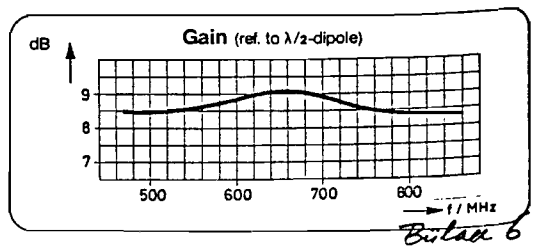

Appendix E: Frequency response channel filter

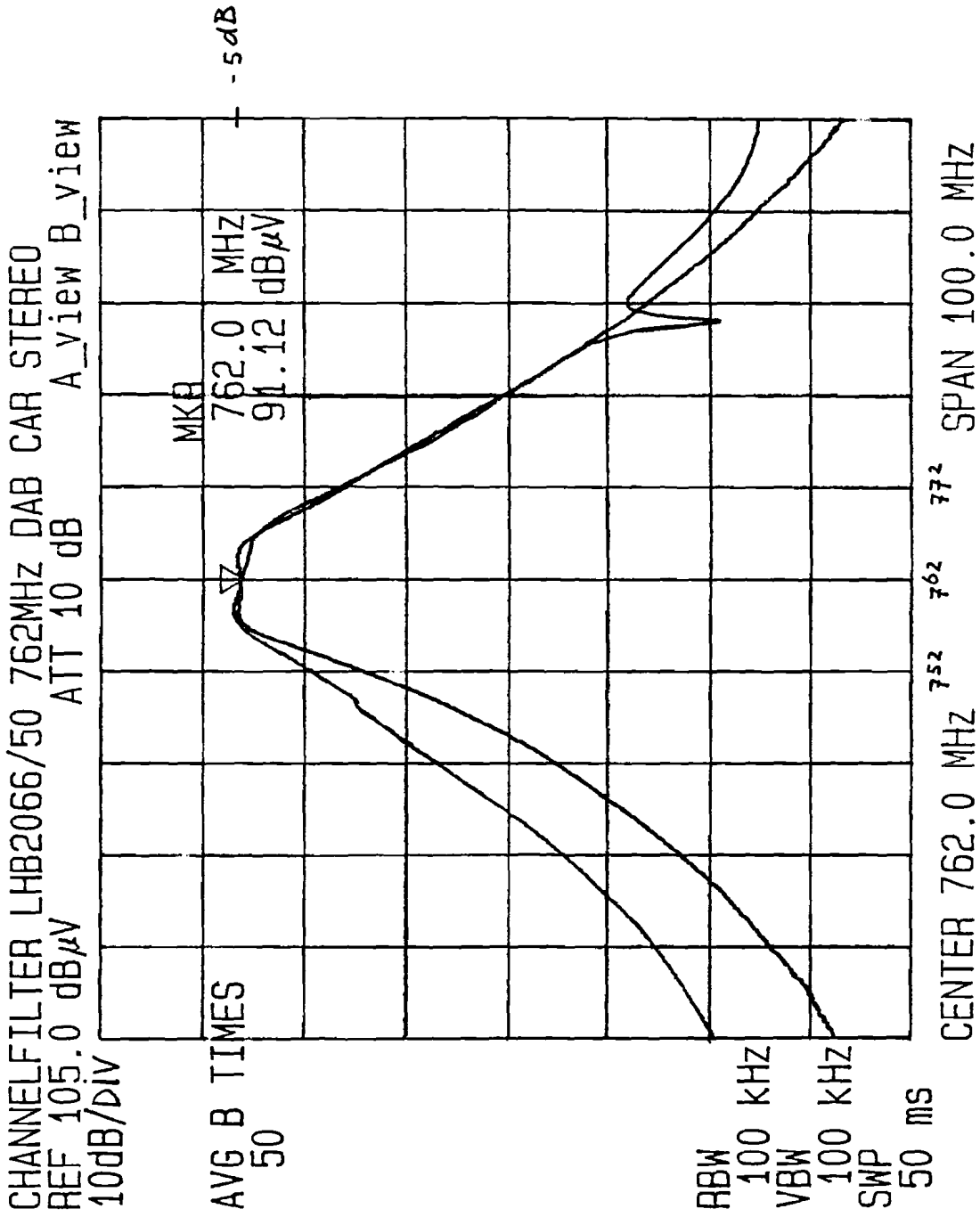

Appendix E: Simulation results Gaussian channel

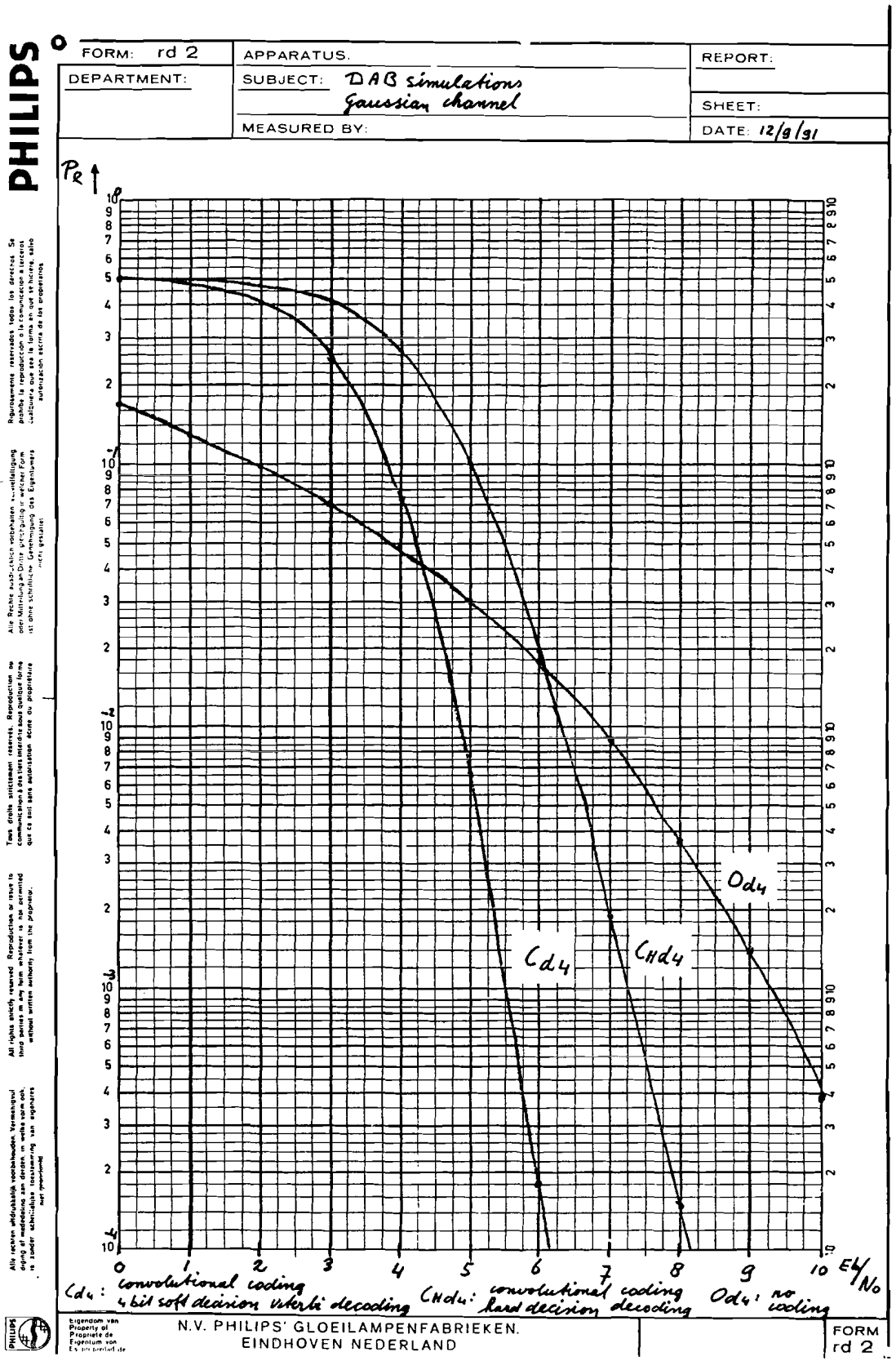

Appendix F: Simulation results Rayleigh channel

F.1 Rayleigh profile 1, no coding

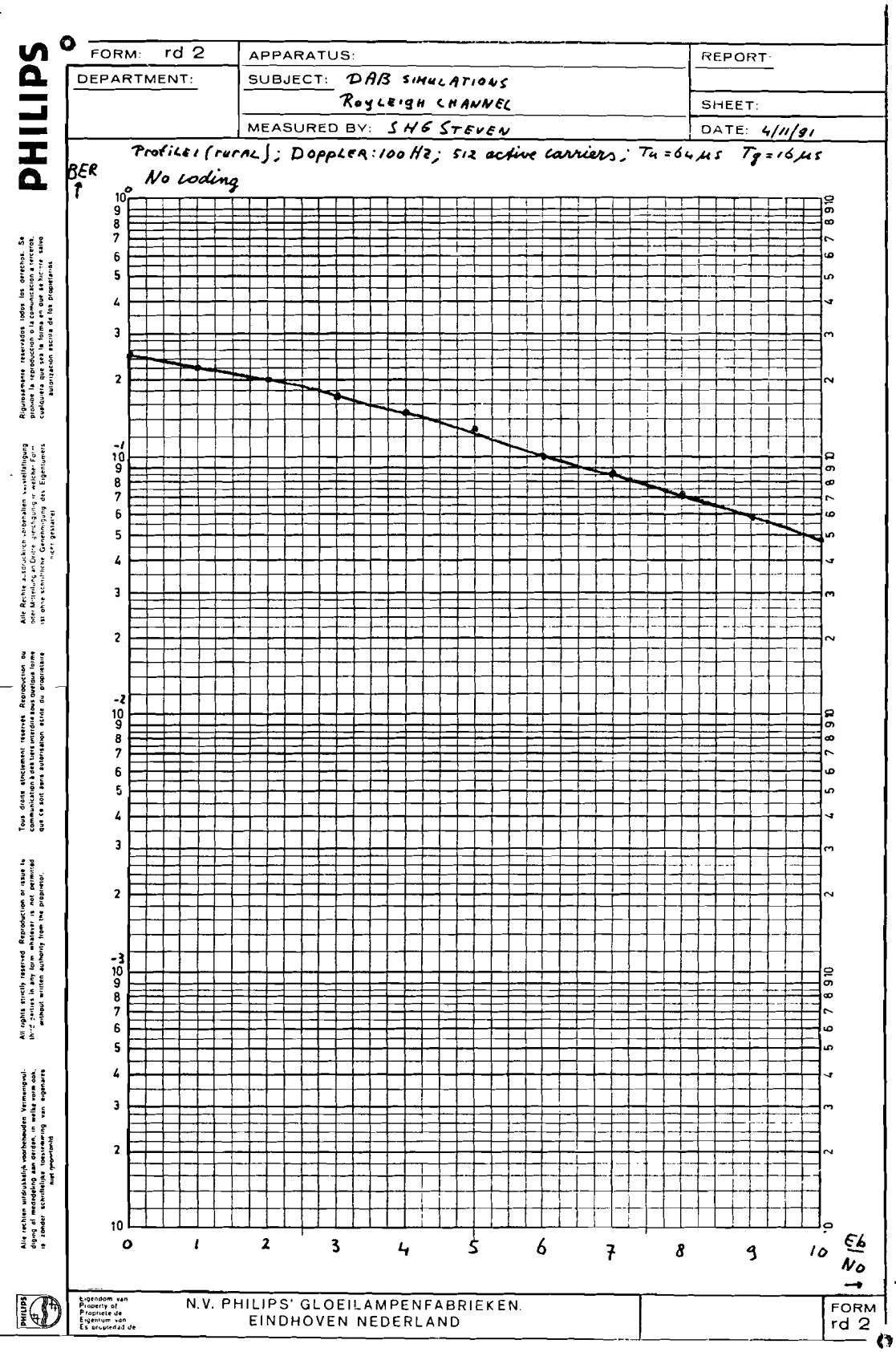

F.2 Rayleigh profile 1, coding

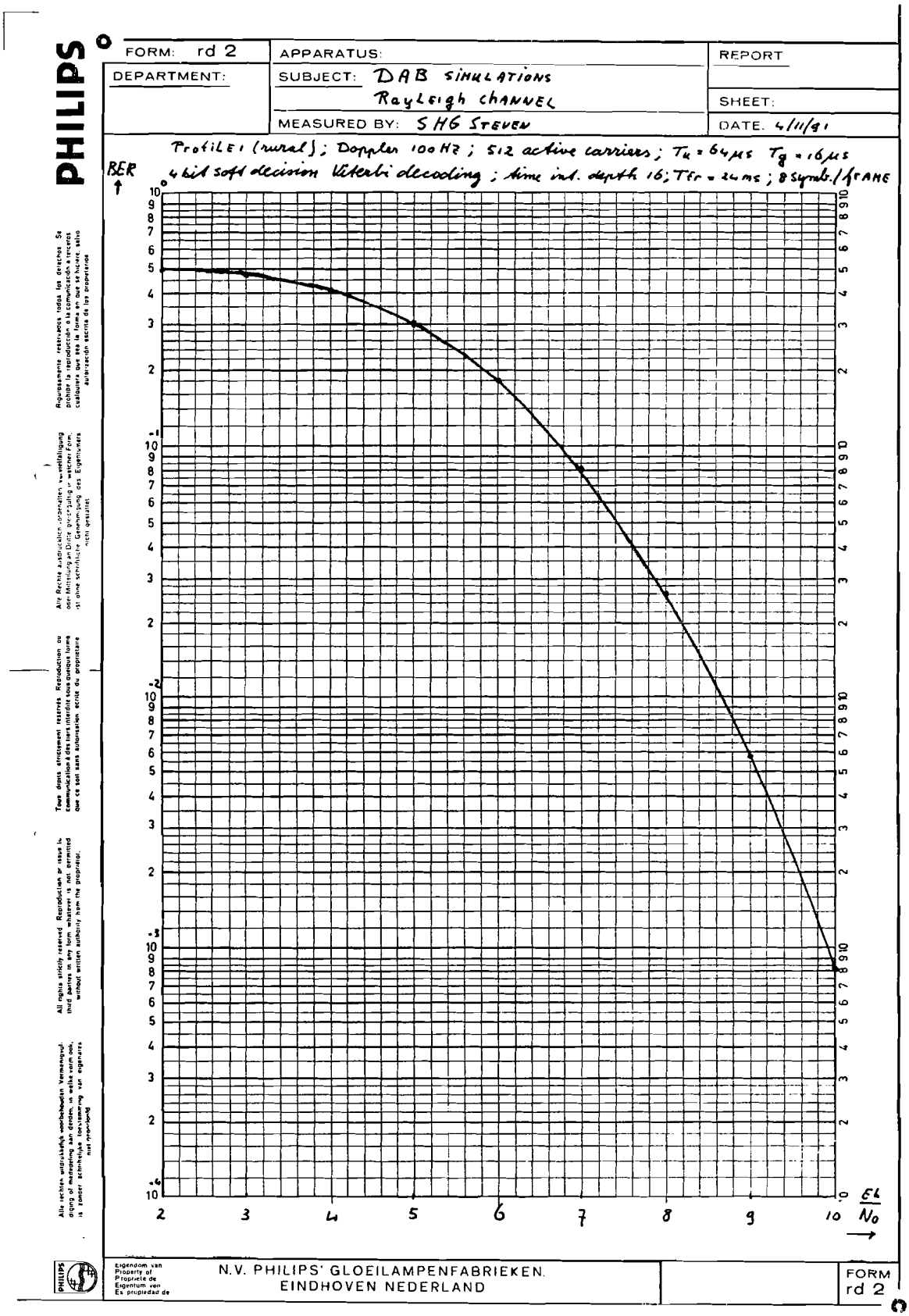

F.3 Rayleigh profile 2, no coding

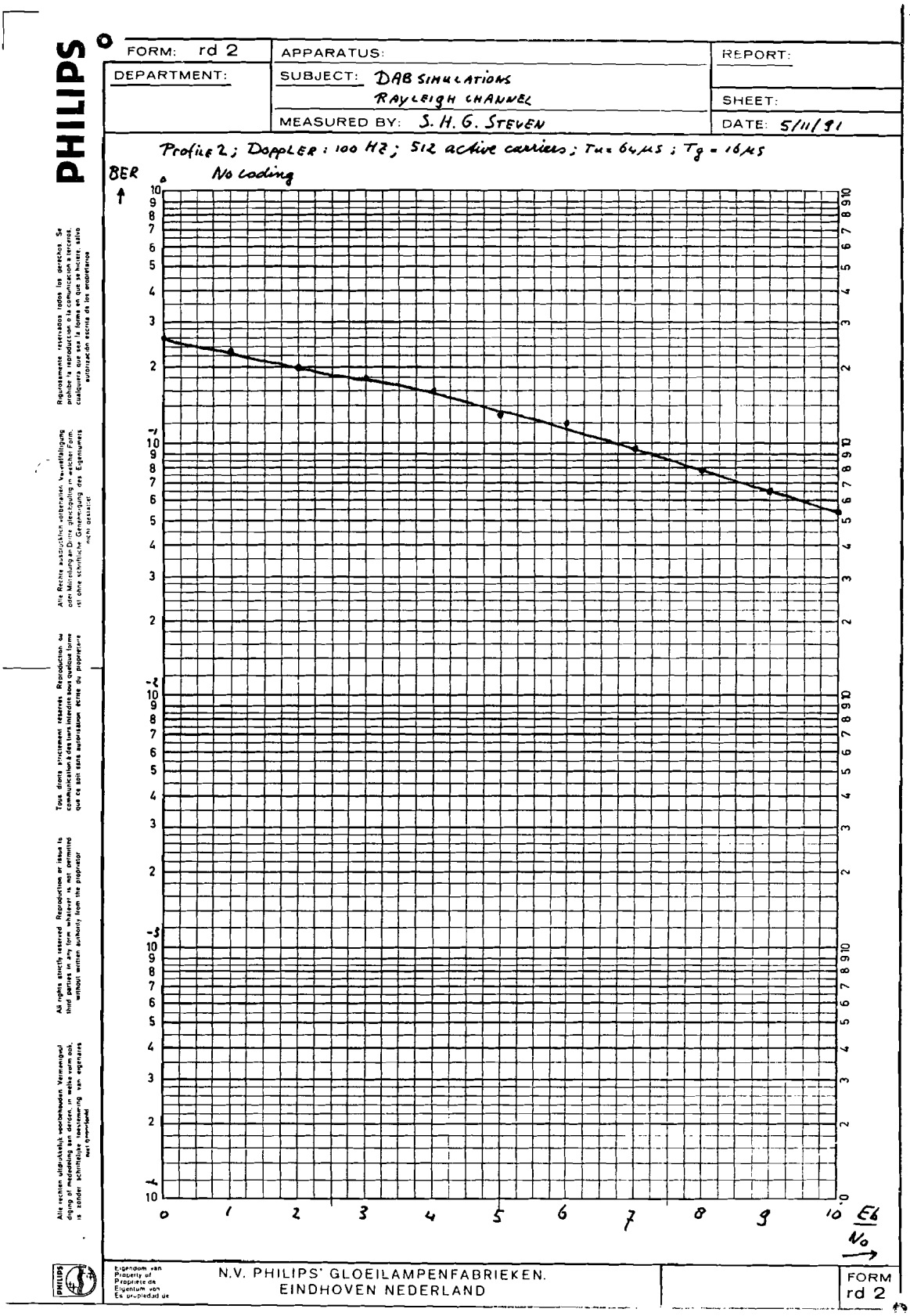

F.4 Rayleigh profile 2, coding

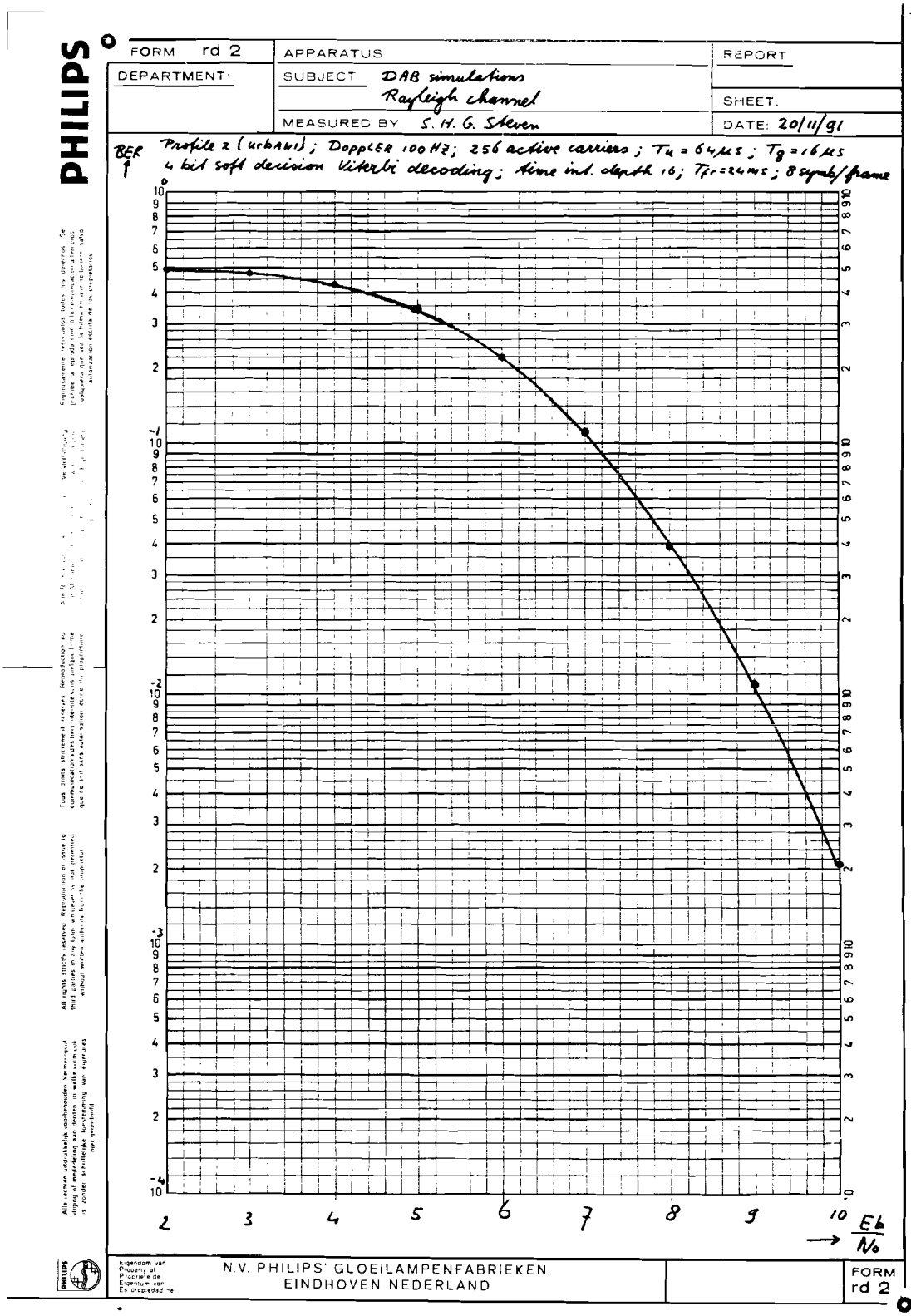

Appendix G: Rayleigh channel profile data

In the program 6 profile models have been implemented. A profile consist of 1, 2 or 3 main reflections (groups). For each main reflection the arrival time is given with respect to the arrival time of the first reflection. The arrival time of the first reflection is set at 0 μs. Each main reflection is provided with its own delay spread. The profiles are normalised, yielding an average power transfer of one. This means the average power at the output of the implemented Rayleigh model is equal to the power at the input of the model. Due to the nature of the Rayleigh channel, the power transfer is a function of time. In the table below the profile data are listed.

Table 3. Profile data.

Profile	group 1			group 2			group 3		
	ampl.	delay	spread	ampl.	delay	spread	ampl.	delay	spread
1(rural)	1.00	0.0	0.11	-	-	-	-	-	-
2(urban1)	1.00	0.0	1.00	-	-	-	-	-	-
3(urban2)	0.66	0.0	1.00	0.34	5	1.00	-	-	-
4(hilly1)	0.91	0.0	0.28	0.09	15	1.00	-	-	-
5(hilly2)	0.33	0.0	0.33	0.50	30	2.00	0.17	80	1.00
6(hilly3)	0.20	0.0	0.33	0.60	20	5.00	0.20	40	0.66

Plots of the impulse responses of the profiles 1 and 2 are given in figure 28 and figure 29.

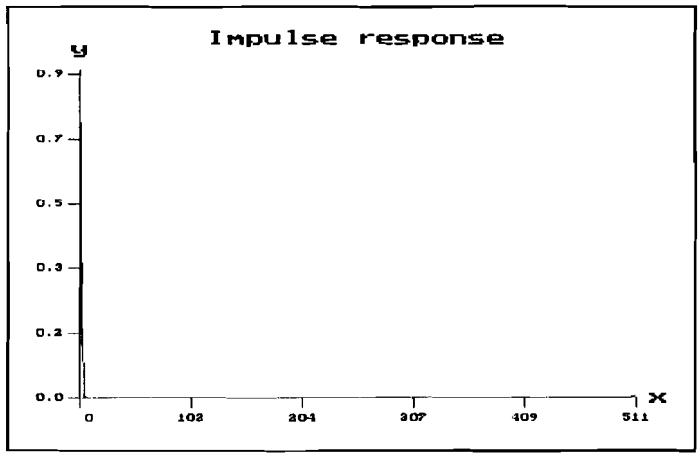

Figure 28. Impulse response profile 1.

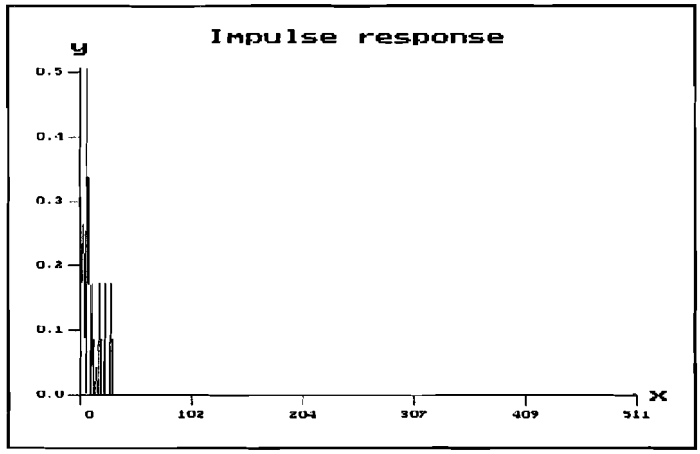

Figure 29. Impulse response profile 2.

These impulse responses are calculated according to the method described in Appendix G. This method has been implemented in the program. The results of this method are very similar to the results obtained if a real impulse is fed through the Rayleigh channel model. The duration (0-511) is 64 μs. The corresponding frequency transfer functions are given in figure 30 and figure 31.

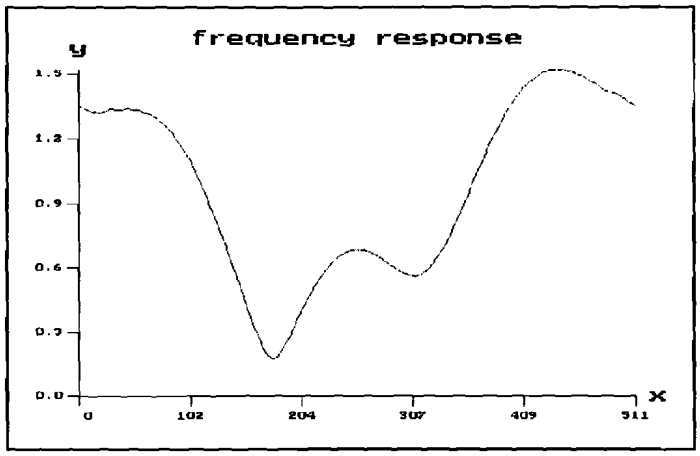

Figure 30. Frequency response profile 1.

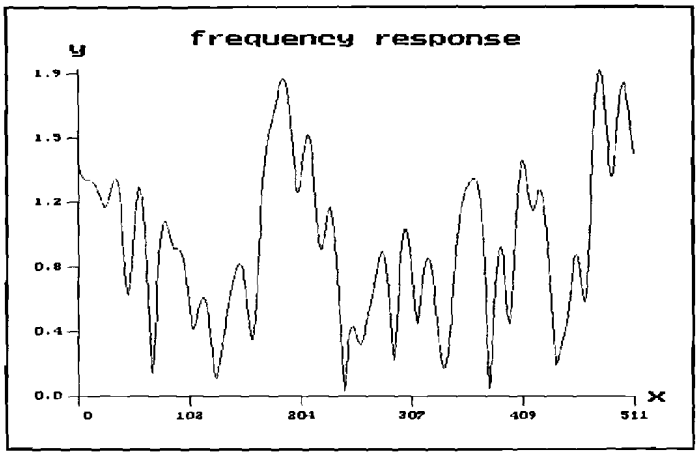

Figure 31. Frequency response profile 2.

The amplitude of the received carriers has been calculated in order to obtain the frequency response. The carriers are numbered from 0 to 511. The occupied bandwidth is 8 MHz. These plots are of course snapshots, since the channel transfer function alters as a function of time.

The plots show that short delay times cause flat fading. With increasing delay times the fades become smaller and more frequent. This is the reason why the stationary reception in case of a single path (for instance in a forest) is, paradoxically, the most critical case, because a deep fade may occur throughout all the band.

Appendix G: Calculation of the impulse response

The impulse response is calculated in the DAB-receiver by calculating an IFFT of the frequency transfer function of the mobile channel. The calculation of the frequency transfer function is based on the phases of the received sine sweep symbol. The transmitted phases of the sine sweep symbol are known at the receiver. Assume that the transmitted phase of carrier number i (frequency f_i) is z_i. The frequency transfer function at frequency f_i is given by

$$H(f_i) = \rho_i e^{j\varphi_i} \tag{44}$$

The received carrier can be written as

$$H(f_i) z_i = \rho_i z_i e^{j\varphi_i} \tag{45}$$

The frequency response may be calculated by

$$H(f_i) = \rho_i z_i e^{j\varphi_i} z_i^* = c\,\rho_i e^{j\varphi_i} \tag{46}$$

This calculation is carried out for each carrier. The impulse response is calculated by taking the IFFT of the frequency responses and by taking the modulus of the result of the IFFT operation. The result is a time discrete version of the impulse response. The calculation method is graphically depicted in figure 32.

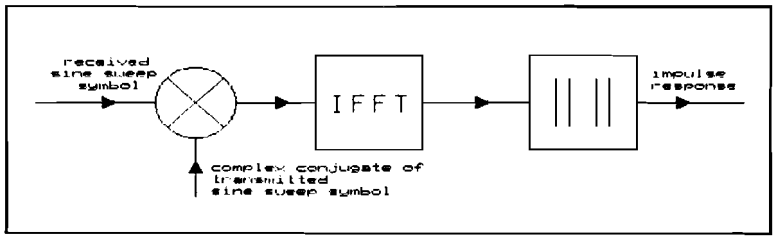

Figure 32. Calculation of the impulse response.

The resolution obtained in the DAB-receiver is given by 64 μs/512 = 0.125 μs.

Appendix H: Channel BER measurement by re-encoding

H.1 Principles of re-encoding

The channel BER can be measured by re-encoding the data at the output of the Viterbi decoder. The re-encoded data are compared with the code bits at the input of the Viterbi decoder and an error is detected if a decoder input code bit is not equal to the corresponding re-encoded bit. It is clear that this method is reliable in the case of a high E_b/N_o: due to the coding gain, the BER at the output of the decoder is considerably lower then the BER at the input of the decoder. The decoded data bits are than a good reference, since the decoded data bits are virtually equal to the bits at the input of the encoder.

The quality of this method may be endangered if the BER at the output of the decoder is comparable to or higher than the BER at the input of the decoder. This event occurs if the E_b/N_o is low.

In order to examine the performance of this method some simulations have been done for a Gaussian channel and a Rayleigh channel. The results are presented in Appendices H.2, H.3 and H.4 (Gaussian channel and two Rayleigh channel profiles). The deviation in the channel BER for a low E_b/N_o is less than a factor 2.

The conclusion is that this method is a reliable method for measuring a channel BER up to 10^{-1}. This is the most important region in the field trial, since the audio decoder fails if the channel BER is above 10^{-1}.

It should be mentioned that the performance of this method for measuring the channel BER in a Rayleigh channel is dependent on the parameters of the DAB-system in use. For instance a reduction of the time interleaving depth or the use of hard decision decoding could influence the performance of this

method and then the reliability of this method should be proven again.

H.2 Re-encoding simulations Gaussian channel

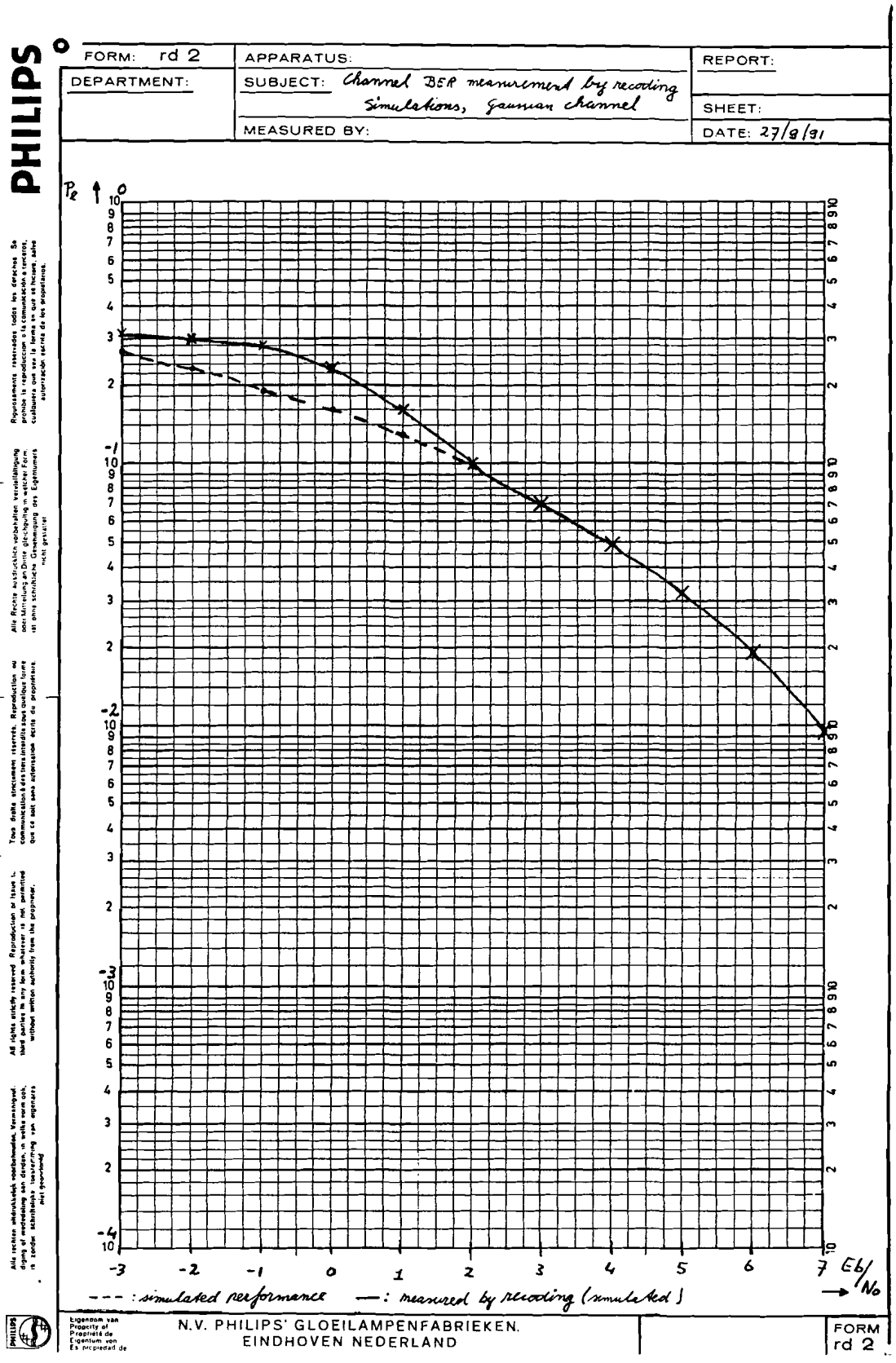

H.3 Re-encoding simulations Rayleigh channel (profile 1)

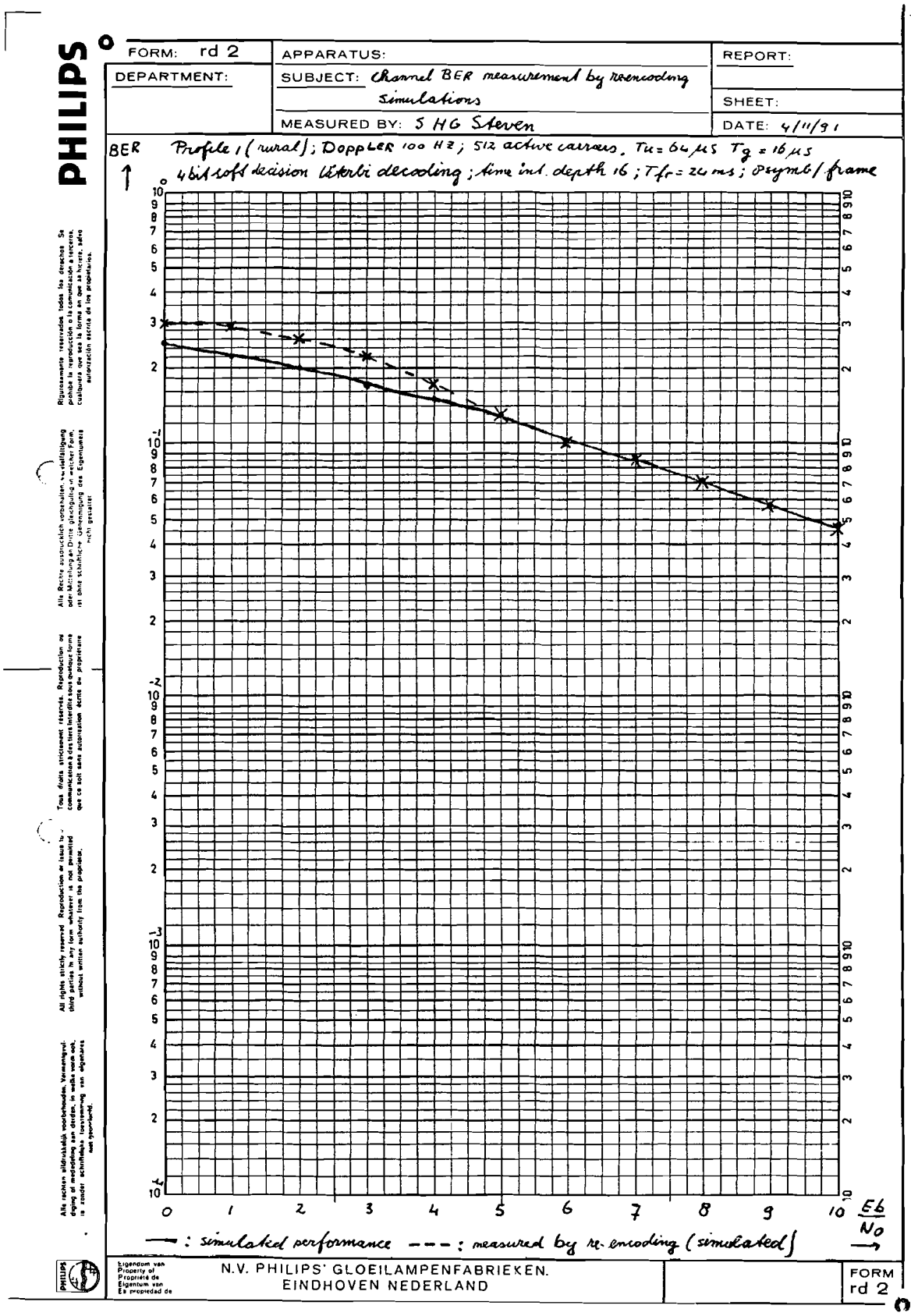

H.4 Re-encoding simulations Rayleigh channel (profile 2)

PHILIPS

FORM: rd 2 | APPARATUS: | REPORT:

DEPARTMENT: | SUBJECT: Channel BER measurement by re-encoding Simulations | SHEET:

MEASURED BY: S. H G. Steven | DATE: 5/11/91

Profile 2 (urban 1); DOPPLER: 100 Hz; 512 active carriers, Tu = 64 μs; Tg = 16 μs
4 bit soft decision Viterbi decoding; time int. depth 16; T_f = 24 ms; 8 symb/frame

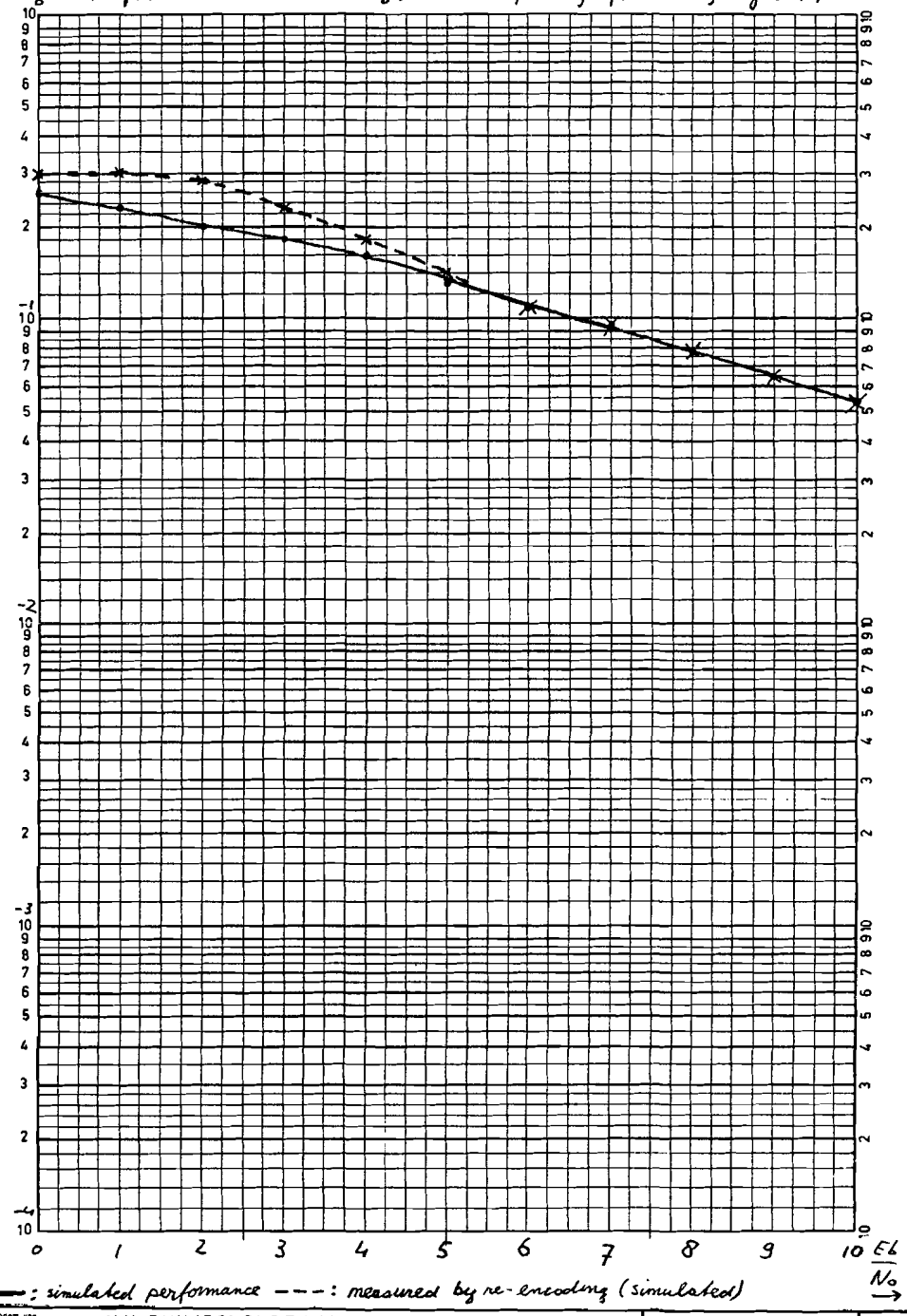

N.V. PHILIPS' GLOEILAMPENFABRIEKEN.
EINDHOVEN NEDERLAND

FORM rd 2

Appendix I: error detector

I.1 Circuit diagram

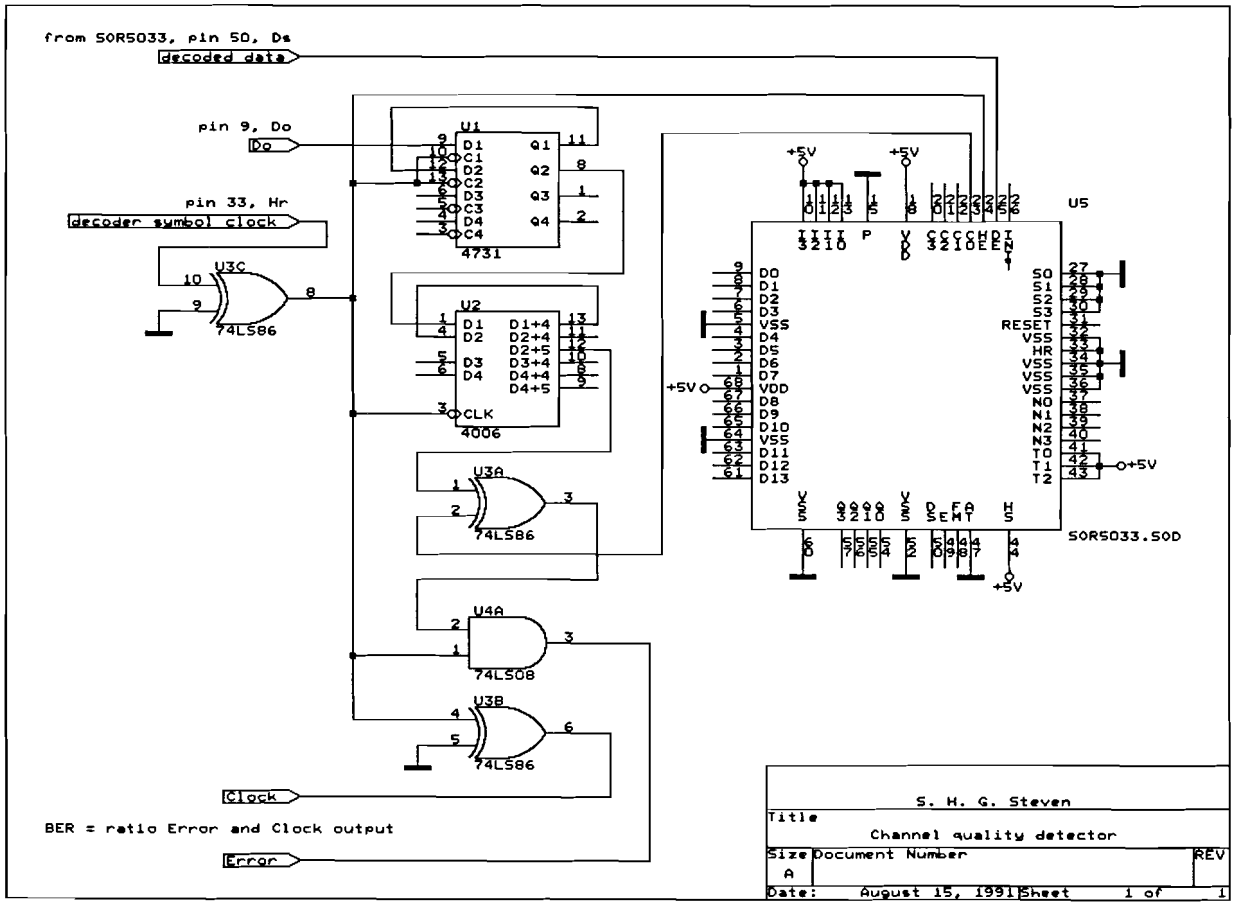

I.2 Description

The output of the Viterbi decoder in the DAB-receiver (from now on referred to as decoder) is re-encoded. This is done by connecting the output of the decoder to the input of a convolutional encoder (U5). The convolutional encoder is functional equivalent to the encoder in the transmitter. The input decoder (Do) is fed through a delay of 137 (128+9) cycles of the decoder symbol clock. This is necessary in order to compensate the delay in the decoder. U1 and U2 are shift registers used to carry out this delay. The re-encoded data and the data the output of the shift register is compared by the exclusive-or gate (U3A). U4A halves the duration of an error pulse, since otherwise successive errors would produce one long pulse. U3B is a clock output buffer. U3C is a clock input buffer.

The clock and error outputs are connected to a counter which calculates the ratio between error and clock frequency. This result represents the channel BER, ie the BER at the input of the decoder.

Appendix J: Modem for synchronisation signals

J.1 Circuit diagram

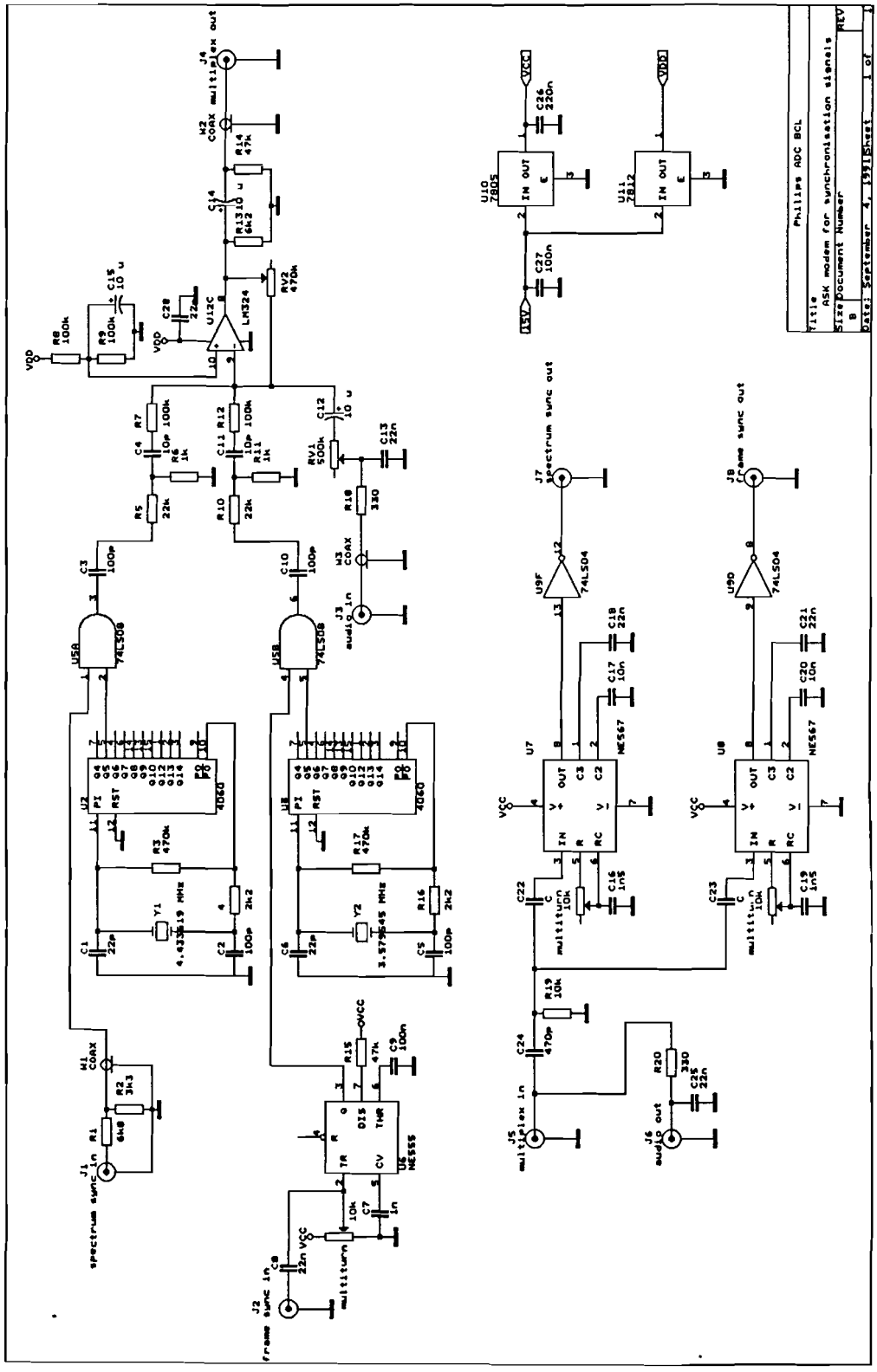

J.2 Description

The modem is an ASK modem, but the data are not random in this case. ASK modulation is used, since it is relatively easy to implement. The upper part of the circuit diagram is the modulator part and the lower part is the demodulator part.

modulator

U2 and U3 are oscillator/dividers. They generate the two carrier frequencies 111.86 and 138.55 kHz (pin 5). U5A and U5B are used for keying the carriers. (This also could be done by switching the oscillators on and off, but this causes erroneous detection pulses in the PLL demodulation process). The frame sync is not a rectangular pulse, but a short negative going peak (the frame sync at the front of the DAB-receiver should be used, the frame sync at the back is unreliable). Therefore this peak is used as a trigger for a monostable multivibrator in order to produce a rectangular pulse. The spectrum sync should be 15 Volt. The audio signal is fed through a low pass filter, since interference at the carrier frequencies (for instance digital pollution on the audio line) may cause errors in the demodulation of the synchronisation signals. The filtered audio signal and the synchronisation signals are multiplexed by the operational amplifier. The synchronisation signals are not sinusoidal but rectangular pulses. However, filtering is not necessary, since the input of the racal recorder is provided with a lowpass filter.

demodulator

The multiplex input is fed through a lowpass filter (R20,C25). The output of this filter is the audio signal. The multiplex input is also fed through a highpass filter in order to remove the audio signal. The output of the highpass filter is connected to two PLL tone detectors (U7 and U8). They perform the demodulation of the two carriers. The synchronisation signal are buffered (U9F and U9D). The multiturns are used for adjusting the initial VCO frequency.

Appendix K: User manual for the simulation program

The simulation program simulates the performance of the COFDM system. The simulations are carried out in baseband. The program performs the coding/ decoding-, time & frequency interleaving/de-interleaving and differential modulation/demodulation algorithms. The transmitted signal is a time discrete version of an OFDM baseband signal. This signal corresponds to the signal at the output of the IFFT in a real transmitter. The user can simulate the performance of the COFDM system in case of various Rayleigh channel models or a Gaussian channel model.

The simulation program consist of four Pascal files:

1. 'Dabsim.pas': the main program.
2. 'Dsp.pas': contains mathematic procedures, (I)FFT procedures, procedures for drawing graphs.
3. 'Monitor.pas': user I/O procedures.
4. 'Raylchan.pas': Rayleigh channel modelling.

An additional file named 'dab.xmt' should be present. The program uses this file to generate a binary sequence, which is used as an input to the encoder, by converting each ASCII character to an 8 bit word.

In general the user needs not to alter the sources files since the user is asked to enter a number of simulation parameters, unless he wants to change one of the following parameters:

1. The number of (active) carriers.
2. The useful symbol duration.
3. The guard interval duration.
4. The frame structure.
5. The number of simulated symbols.

After the program has been started the user is asked to enter a number of parameters. In figure 33 a example of an input session is given:

```
Graphics display of reference symbol and impulse response [Y/N] ? N
Rayleigh channel [Y/N] ? Y
Enter profile number,
 [1=rural, 2=urban1, 3=urban2, 4=hilly1, 5=hilly2, 6=hilly3]: 1
Enter Doppler frequency [0..500 Hz]: 100
Additive white gaussian noise [Y/N] ? Y
Enter start value of Eb/No (integer) : 6
Enter stop value of Eb/No (integer) : 8
Use of convolutional coding [Y/N] ? Y
Use of time interleaving [Y/N] ? Y
Use of frequency interleaving [Y/N] ? Y
Use of guard interval [Y/N] ? Y

All correct [Y/N] ?
```

Figure 33. Example of an input session.

If the first question is answered with 'Y' then the impulse response and the frequency transfer function of the channel is calculated and graphically depicted. This calculation is based on the received sine sweep symbol. Of course the result of the calculation is a snapshot in a Rayleigh channel.

If the user wants a Rayleigh channel, then he is asked to enter a profile and the maximum doppler shift (D_{max} in (34)). If the user chooses for Gaussian noise then he is asked to specify a range of E_b/N_o values. These values must be integers. If the user wants to simulate only one E_b/N_o, he gives the same value to the start value and the stop value. The meaning of the next four questions is obvious. If the user made a mistake during the input session he may start a rerun of the input session by answering 'N' to the last question.

After some initial calculations the screen looks like this:

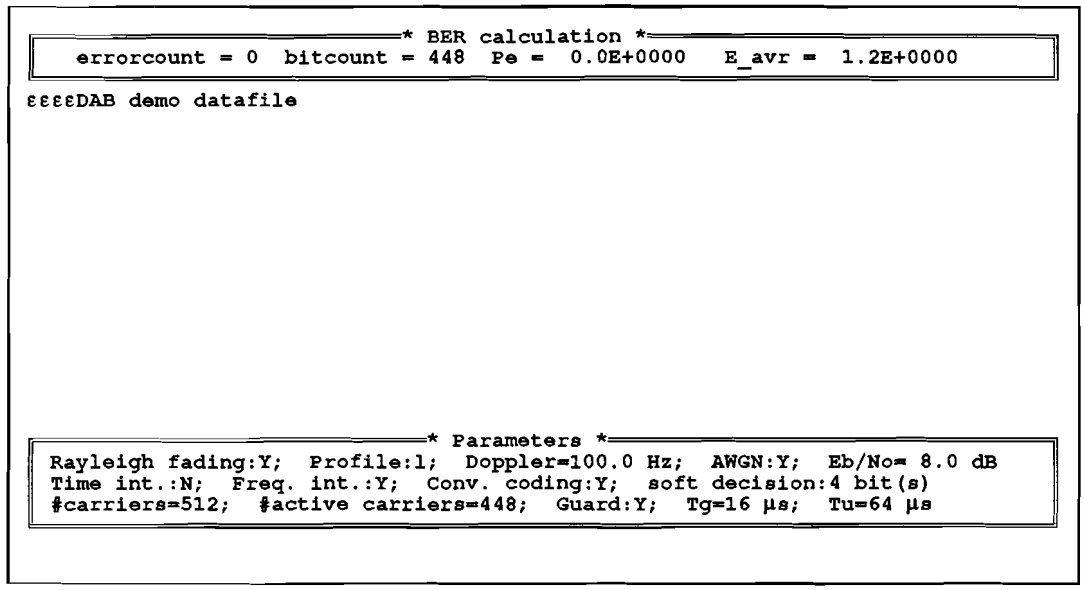

Figure 34. simulation output screen.

In the upper window the number of simulated and erroneous bits (at the output of the Viterbi decoder) is given. The BER at the output of the Viterbi decoder is given too. The last parameter contains information about the energy transfer of the Rayleigh and/or Gaussian channel. 'E_avr' is the mean energy at the output of the Rayleigh and/or Gaussian channel divided by the energy at the input of the channel. If E_b/N_o is 0 dB then 'E_avr' becomes 2 after a sufficiently long simulation time. This parameter is helpful in order to get an indication whether the simulation time is sufficient or not.

The lower window contains the parameters of the simulated DAB-system and the parameters of the channel model used. There is no information about the frame structure.

Between the two windows mentioned above, the received and decoded datafile is written. The most meaningful result appears here, provided that 'dab.xmt' is an ASCII text file. If one is interested in the BER, it is advisable to use a random datafile since the data bits of an ASCII file may be not random enough.

The results of the simulations, together with the parameters of the simulated system and the parameters of the channel are written to an output file ('dab.out') at the end of the simulations.